Signs of composite Higgs pair production at next-to-leading order

R. Gröber,[a] **M. Mühlleitner**[b] **and M. Spira**[c]

[a]*INFN, Sezione di Roma Tre,*
Via della Vasca Navale 84, I-00146 Roma, Italy

[b]*Institute for Theoretical Physics, Karlsruhe Institute of Technology,*
Wolfgang-Gaede-Str. 1, 76131 Karlsruhe, Germany

[c]*Paul Scherrer Institute,*
CH-5323 Villigen PSI, Switzerland

E-mail: groeber@roma3.infn.it, milada.muehlleitner@kit.edu, michael.spira@psi.ch

ABSTRACT: In composite Higgs models the Higgs boson arises as a pseudo-Goldstone boson from a strongly-interacting sector. Fermion mass generation is possible through partial compositeness accompanied by the appearance of new heavy fermionic resonances. The Higgs couplings to the Standard Model (SM) particles and between the Higgs bosons themselves are modified with respect to the SM. Higgs pair production is sensitive to the trilinear Higgs self-coupling but also to anomalous couplings like the novel 2-Higgs-2-fermion coupling emerging in composite Higgs models. The QCD corrections to SM Higgs boson pair production are known to be large. In this paper we compute, in the limit of heavy loop particle masses, the next-to-leading order (NLO) QCD corrections to Higgs pair production in composite Higgs models without and with new heavy fermions. The relative QCD corrections are found to be almost insensitive both to the compositeness of the Higgs boson and to the details of the heavy fermion spectrum, since the leading order cross section dominantly factorizes. With the obtained results we investigate the question if, taking into account Higgs coupling constraints, new physics could first be seen in Higgs pair production. We find this to be the case in the high-luminosity option of the LHC for composite Higgs models with heavy fermions. We also investigate the invariant mass distributions at NLO QCD. While they are sensitive to the Higgs non-linearities and hence anomalous couplings, the influence of the heavy fermions is much less pronounced.

KEYWORDS: Beyond Standard Model, Higgs Physics, Perturbative QCD, Technicolor and Composite Models

ARXIV EPRINT: 1602.05851

Contents

1 Introduction

The LHC Higgs data of Run 1 suggest that the scalar particle observed by the LHC experiments ATLAS and CMS in 2012 [1–4] is compatible with the Higgs boson of the Standard Model (SM). The non-vanishing vacuum expectation value (VEV) v of the SU(2) Higgs doublet field ϕ in the ground state is crucial for the mechanism of electroweak symmetry breaking (EWSB) [5–9]. It it is induced by the Higgs potential

$$V = \lambda \left[\phi^\dagger \phi - \frac{v^2}{2} \right]^2 . \tag{1.1}$$

Introducing the Higgs field in the unitary gauge, $\phi = (0, [v + H]/\sqrt{2})^T$, it reads

$$V = \frac{M_H^2}{2} H^2 + \frac{\lambda_{HHH}}{3!} H^3 + \frac{\lambda_{HHHH}}{4!} H^4 . \tag{1.2}$$

In the SM the trilinear and quartic Higgs self-couplings are uniquely determined in terms of the Higgs boson mass $M_H = \sqrt{2\lambda}v$,

$$\lambda_{HHH} = \frac{3M_H^2}{v} \qquad \text{and} \qquad \lambda_{HHHH} = \frac{3M_H^2}{v^2} , \tag{1.3}$$

with $v \approx 246\,\text{GeV}$. The experimental verification of the form of the Higgs potential through the measurement of the Higgs self-couplings is the final step in the program aimed to test the mechanism of EWSB. The Higgs self-couplings are accessible in multi-Higgs production processes [10–13]. While previous studies [14–33] showed that the probe of the trilinear Higgs self-coupling in Higgs pair production should be possible at the high-luminosity LHC, although it is experimentally very challenging, the quartic Higgs self-interaction is out of reach. The cross section of triple Higgs production giving access to this coupling suffers from too low signal rates fighting against a large background [11, 13, 34–37]. The relations in eq. (1.3) do not hold in models beyond the SM (BSM), and this would manifest itself in

the Higgs pair production process. In general, however, new physics (NP) not only affects the value of the Higgs self-coupling, but also other couplings involved in the Higgs pair production process.[1] An approach that allows to smoothly depart from the SM in a consistent and model-independent way is offered by the effective field theory (EFT) framework based on higher dimensional operators which are added to the SM Lagrangian with coefficients that are suppressed by the typical scale Λ where NP becomes relevant [39–43]. These higher dimensional operators modify the couplings involved in Higgs pair production, such as the trilinear Higgs self-coupling and the Higgs Yukawa couplings. Additionally they give rise to novel couplings, like a 2-Higgs-2-fermion coupling, that can have a significant effect on the process. While the trilinear Higgs self-coupling has not been delimited experimentally yet,[2] the Higgs couplings to the SM particles have been constrained by the LHC data and in particular the Higgs couplings to the massive gauge bosons. An interesting question to ask is, while taking into account the information on the Higgs properties gathered at the LHC, if it could be that despite the Higgs boson behaving SM-like, we see NP emerging in Higgs pair production? And if so, could it even be, that we see NP before having any other direct hints e.g. from new resonances or indirect hints from e.g. Higgs coupling measurements?

Previous works have applied the EFT approach to investigate BSM effects in Higgs pair production.[3] A study of the effects of genuine dimension-six operators in Higgs pair production can be found in ref. [79]. Anomalous couplings in Higgs pair production have been investigated in [80–83]. In [84–86] the EFT was applied to investigate the prospects of probing the trilinear Higgs self-coupling at the LHC. Reference [87] on the other hand addressed the question on the range of validity of the EFT approach for Higgs pair production by using the universal extra dimension model.

The dominant Higgs pair production process at the LHC is gluon fusion, $gg \rightarrow HH$, which is mediated by loops of heavy fermions. It can be modified due to NP via deviations in the trilinear Higgs self-coupling, in the Higgs to fermion couplings, via new couplings such as a direct coupling of two fermions to two Higgs bosons, new particles like e.g. heavy quark partners in the loop, or additional (virtual) Higgs bosons, splitting into two lighter final state Higgs bosons. The purpose of this paper is to address the question of whether it will be possible to see deviations from the SM for the first time in non-resonant Higgs pair production processes by considering explicit models. It has been found that large deviations from SM Higgs pair production can arise in composite Higgs models, which is mainly due to the novel 2-Higgs-2-fermion coupling [47, 88]. In this paper, we will hence focus on this class of models. We assume that no deviations with respect to the SM are seen in any of the LHC Higgs coupling analyses, i.e. that the deviations in the standard Higgs couplings due to NP are below the expected experimental sensitivity, for the case of the LHC high-energy Run 2 and for the high-luminosity option of the LHC. Additionally, we assume that no NP will

---

[1]Note, however, that in ref. [38] a model is discussed, where only the Higgs self-couplings are modified with respect to the SM via loop corrections of an invisible new state.

[2]In some NP models, the trilinear Higgs self-coupling can still deviate significantly from the SM expectations [44–46].

[3]For effects of NP on the trilinear Higgs self-coupling and/or Higgs pair production within specific BSM models in recent studies, see e.g. [44–78].

be observed in direct searches or indirect measurements. The prospects of NP emerging from composite Higgs models for the first time in non-resonant Higgs pair production from gluon fusion are analyzed under these conditions. Our analysis is complementary to previous works [58, 89], which focused on deviations in Higgs pair production due to modifications in the trilinear Higgs coupling. In ref. [89] the question is investigated on how well the trilinear Higgs coupling needs to be measured in various scenarios to be able to probe NP. The main focus of ref. [58] is on how to combine a deviation in the trilinear Higgs coupling with other Higgs coupling measurements to support certain BSM extensions.

Gluon fusion into Higgs pairs exhibits large QCD corrections. In ref. [10], the next-to-leading order (NLO) QCD corrections were computed in the large top mass approximation and found to be of $\mathcal{O}(90\%)$ at $\sqrt{s} = 14 \, \text{TeV}$ for a Higgs boson mass of $125 \, \text{GeV}$. The effects of finite top quark masses have been analyzed in [48, 90–94]. While the $m_t \to \infty$ approximation exhibits uncertainties of order 20% on the leading order (LO) cross section at $\sqrt{s} = 14 \, \text{TeV}$ for a light Higgs boson [88, 95, 96] and badly fails to reproduce the differential distributions [16], the uncertainty on the K-factor, i.e. the ratio between the loop-corrected and the LO cross section, is much smaller due to the fact that in the dominant soft and collinear contributions the full LO cross section can be factored out. The next-to-next-to-leading order (NNLO) corrections have been provided by [97–99] in the heavy top mass limit. The finite top mass effects have been estimated to be of about 10% at NLO and $\sim 5\%$ at NNLO [100]. Soft gluon resummation at next-to-leading logarithmic order has been performed in [101] and has been extended recently to the next-to-next-to-leading logarithmic level in [102]. First results towards a fully differential NLO calculation have been provided in [92, 94]. For a precise determination of the accessibility of BSM effects in gluon fusion to a Higgs pair, the NLO QCD corrections are essential and need to be computed in the context of these models. They have been provided in the large loop particle mass limit for the singlet-extended SM [71], for the 2-Higgs-doublet model [60] and for the MSSM [10, 77].[4] In the same limit, the NLO QCD corrections including dimension-6 operators have been computed in [103]. In this work, we calculate for the first time the NLO QCD corrections in the large loop particle mass limit for models with vector-like fermions such as composite Higgs models.

The paper is organized as follows. In section 2 we briefly introduce composite Higgs models. In section 3 we present the NLO QCD corrections to the gluon fusion process in the framework of composite Higgs models including vector-like fermions. In the subsequent sections we analyze whether a possible deviation from the SM signal could be seen or not at the LHC Run 2 with an integrated luminosity of $300 \, \text{fb}^{-1}$ and/or the high-luminosity LHC with an integrated luminosity of $3000 \, \text{fb}^{-1}$ for different models: in section 4 for the composite Higgs models MCHM4 and MCHM5, and in section 5 for a composite Higgs model with one multiplet of fermionic resonances below the cut-off. In section 6 we discuss the invariant mass distributions with and without the inclusion of the new fermions. We conclude in section 7.

---

[4]Reference [77] also shows how the provided results can be adapted to the Next-to-Minimal Supersymmetric extension of the SM.

2 Composite Higgs models

In composite Higgs models the Higgs boson arises as a pseudo-Nambu Goldstone boson of a strongly interacting sector [104–112]. A global symmetry is broken at the scale f to a subgroup containing at least the SM gauge group. The new strongly-interacting sector can be characterized by a mass scale m_ρ and a coupling g_ρ, with $f = m_\rho/g_\rho$. An effective low-energy description of such models is provided by the Strongly Interacting Light Higgs (SILH) Lagrangian [113], which, in addition to the SM Lagrangian, contains higher dimensional operators including the SM Higgs doublet ϕ to account for the composite nature of the Higgs boson. Listing only the operators relevant for Higgs pair production by gluon fusion, the SILH Lagrangian reads[5]

$$\mathcal{L}^{\text{SILH}} \supset \frac{c_H}{2f^2} \partial^\mu \left(\phi^\dagger \phi\right) \partial_\mu \left(\phi^\dagger \phi\right) - \frac{c_6 \lambda}{f^2} \left(\phi^\dagger \phi\right)^3$$
$$+ \left[\left(\frac{c_u y_u}{f^2} \phi^\dagger \phi \, \overline{Q}_L \phi^c u_R + \frac{c_d y_d}{f^2} \phi^\dagger \phi \, \overline{Q}_L \phi d_R\right) + \text{h.c.}\right]$$
$$+ \frac{c_g \alpha_s}{4\pi f^2} \frac{y_t^2}{g_\rho^2} \phi^\dagger \phi \, G_{\mu\nu}^a G^{a\mu\nu} , \qquad (2.1)$$

with the Yukawa couplings $y_q = \sqrt{2} m_q/v$ $(q = u, d)$, where m_q denotes the quark mass, λ the quartic Higgs coupling and $\alpha_s = g_s^2/(4\pi)$ the strong coupling constant in terms of the $\text{SU}(3)_c$ gauge coupling g_s.[6] Here Q_L denotes the left-handed quark doublet. The effective Lagrangian accounts for several effects that can occur in Higgs pair production via gluon fusion in composite Higgs models: a shift in the trilinear Higgs self-coupling and in the Higgs couplings to the fermions, a novel coupling of two fermions to two Higgs bosons and additional new fermions in the loops. The latter effect is encoded in the effective operator with the gluon field strength tensors $G_{\mu\nu}$ coupling directly to the Higgs doublet ϕ. While the SILH Lagrangian eq. (2.1) is a valid description for small values of $\xi = (v/f)^2$, larger values require a resummation of the series in ξ. This is provided by explicit models built in five-dimensional warped space. In the Minimal Composite Higgs Models (MCHM) the gauge symmetry $\text{SO}(5) \times \text{U}(1)_X \times \text{SU}(3)$ is broken down to the SM gauge group on the ultraviolet (UV) boundary and to $\text{SO}(4) \times \text{U}(1)_X \times \text{SU}(3)$ on the infrared. The Higgs coupling modifications in these models can be described by one single parameter, given by ξ. For the fermions, they depend on the representations of the bulk symmetry into which the fermions are embedded. In the model MCHM4 based on ref. [115] the fermions transform in the spinorial representation of the global symmetry, in the model MCHM5 based on ref. [116] the fermions transform in the fundamental representation. In table 1 we report the modifications of the Higgs couplings to the SM particles with respect to the corresponding SM couplings in the SILH set-up and in the MCHM4 and MCHM5. The last two lines list the novel couplings not present in the SM, i.e. the 2-Higgs-2-fermion coupling and the effective single and double Higgs couplings to a gluon pair, as defined in

---

[5]We have not included the chromomagnetic dipole moment operator which modifies the interactions between the gluons, the top quark and the Higgs boson and can be expected to be of moderate size [114].

[6]The relation between the coefficients c and the coefficients $\bar{c}$ in eq. (2.1) of ref. [103] is $\bar{c}_x = c_x \xi$ $(x = H, 6)$, $\bar{c}_u = c_u \xi$ and $\bar{c}_g = \alpha_2/(16\pi) y_t^2/g_\rho^2 c_g \xi$ with $\xi = v^2/f^2$ and $\alpha_2 = \sqrt{2} G_F m_W^2/\pi$ in terms of the Fermi constant G_F and the W boson mass m_W.

	SILH	MCHM4	MCHM5
$g_{hVV}/g_{hVV}^{\rm SM}$	$1 - c_H\,\xi/2$	$\sqrt{1-\xi}$	$\sqrt{1-\xi}$
$g_{hf\bar{f}}/g_{hf\bar{f}}^{\rm SM}$	$1 - (c_H/2 + c_y)\,\xi$	$\sqrt{1-\xi}$	$\frac{1-2\xi}{\sqrt{1-\xi}}$
$g_{hhh}/g_{hhh}^{\rm SM}$	$1 + (c_6 - 3c_H/2)\,\xi$	$\sqrt{1-\xi}$	$\frac{1-2\xi}{\sqrt{1-\xi}}$
$g_{hhf\bar{f}}$	$-(c_H + 3c_y)\,\xi\,m_f/v^2$	$-\xi m_f/v^2$	$-4\xi\,m_f/v^2$
g_{hgg} and g_{hhgg}	$3c_g(y_t^2/g_\rho^2)\xi$	0	0

Table 1. Higgs couplings to the SM particles (massive gauge bosons $V \equiv Z, W$ and fermions) and Higgs self-couplings in the SILH set-up, the MCHM4 and MCHM5 normalized to the corresponding couplings in the SM, $g_X/g_X^{\rm SM}$. The last two lines summarize the novel couplings not present in the SM, the 2-Higgs-2-fermion coupling and the effective single and double Higgs couplings to a gluon pair as defined in eqs. (2.2)–(2.4).

the Feynman rules derived from the SILH Lagrangian,

$$hhf\bar{f} \; : \; -ig_{hhf\bar{f}} \tag{2.2}$$

$$hgg \; : \; i\delta^{ab}\frac{\alpha_s}{3\pi v}[k_1^\nu k_2^\mu - (k_1 \cdot k_2)g^{\mu\nu}]g_{hgg} \tag{2.3}$$

$$hhgg \; : \; i\delta^{ab}\frac{\alpha_s}{3\pi v^2}[k_1^\nu k_2^\mu - (k_1 \cdot k_2)g^{\mu\nu}]g_{hhgg} \tag{2.4}$$

where $k_{1,2}$ denote the incoming momenta of the two gluons $g_\mu^a(k_1)$ and $g_\nu^b(k_2)$. The effective gluon couplings are not present in MCHM4 and MCHM5, since we only consider pure Higgs non-linearities whenever we refer to these models.

In composite Higgs models fermion mass generation can be achieved by the principle of partial compositeness [117, 118]. The SM fermions are elementary particles that couple linearly to heavy states of the strong sector with equal quantum numbers under the SM gauge group. In particular the top quark can be largely composite. But also the bottom quark can have a sizeable coupling to heavy bottom partners. For gluon fusion this not only means that new bottom and top partners are running in the loops but mixing effects also induce further changes in the top- and bottom-Higgs Yukawa couplings. In addition to the MCHM4 and 5 models involving only the pure non-linearities of the Higgs boson in the Higgs couplings, we consider a model with heavy top and bottom partners based on the minimal $SO(5) \times U(1)_X/SO(4) \times U(1)_X$ symmetry breaking pattern. The additional $U(1)_X$ is introduced to guarantee the correct fermion charges. The new fermions transform in the antisymmetric representation **10** of SO(5) in this model MCHM10, given by

$$\mathcal{Q} = \frac{1}{2} \times \tag{2.5}$$

$$\begin{pmatrix}
0 & -(u+u_1) & \frac{i(d-\chi)}{\sqrt{2}} + \frac{i(d_1-\chi_1)}{\sqrt{2}} & \frac{d+\chi}{\sqrt{2}} - \frac{d_1+\chi_1}{\sqrt{2}} & d_4 + \chi_4 \\
u_1 + u & 0 & \frac{d_1+\chi_1}{\sqrt{2}} + \frac{d+\chi}{\sqrt{2}} & \frac{i(d_1-\chi_1)}{\sqrt{2}} - \frac{i(d-\chi)}{\sqrt{2}} & -i(d_4 - \chi_4) \\
-\frac{i(d_1-\chi_1)}{\sqrt{2}} - \frac{i(d-\chi)}{\sqrt{2}} & -\frac{d_1+\chi_1}{\sqrt{2}} - \frac{d+\chi}{\sqrt{2}} & 0 & u_1 - u & t_4 + T_4 \\
\frac{d_1+\chi_1}{\sqrt{2}} - \frac{d+\chi}{\sqrt{2}} & \frac{i(\chi_1-d_1)}{\sqrt{2}} + \frac{i(d-\chi)}{\sqrt{2}} & u - u_1 & 0 & -i(t_4 - T_4) \\
-d_4 - \chi_4 & i(d_4 - \chi_4) & -t_4 - T_4 & i(t_4 - T_4) & 0
\end{pmatrix}$$

with the electric charge-2/3 fermions u, u_1, t_4 and T_4, the fermions d, d_1 and d_4 with charge $-1/3$, and the χ, χ_1 and χ_4 with charge 5/3. The coset SO(5)/SO(4) leads to four Goldstone bosons, among which three provide the longitudinal modes of the massive vector bosons $W^\pm$ and Z, and the remaining one is the Higgs boson. The four Goldstone bosons can be parameterized in terms of the field

$$\Sigma = \Sigma_0 \exp(\Pi(x)/f), \qquad \Sigma_0 = (0, 0, 0, 0, 1), \qquad \Pi(x) = -i\sqrt{2}T^{\hat{a}}h^{\hat{a}}(x), \qquad (2.6)$$

with the generators $T^{\hat{a}}$ ($\hat{a} = 1, \ldots, 4$) of the coset SO(5)/SO(4)

$$(T^{\hat{a}})_{ij} = -\frac{i}{\sqrt{2}}\left(\delta_i^{\hat{a}}\delta_j^5 - \delta_j^{\hat{a}}\delta_i^5\right). \qquad (2.7)$$

The generators of the SU(2)$_{L,R}$ in the fundamental representation read ($a, b, c = 1, 2, 3$, $i, j = 1, \ldots, 5$),

$$(T^a_{L/R})_{ij} = -\frac{i}{2}\left[\frac{1}{2}\epsilon^{abc}(\delta_i^b\delta_j^c - \delta_j^b\delta_i^c) \pm \delta_i^a\delta_j^4 \mp \delta_i^4\delta_j^a\right]. \qquad (2.8)$$

The non-linear σ-model describing the effective low-energy physics of the strong sector is given by the Lagrangian

$$\begin{aligned}
\mathcal{L} = {}& \frac{f^2}{2}\left(D_\mu\Sigma\right)\left(D^\mu\Sigma\right)^T + i\,\mathrm{Tr}(\overline{\mathcal{Q}}_R\slashed{D}\mathcal{Q}_R) + i\,\mathrm{Tr}(\overline{\mathcal{Q}}_L\slashed{D}\mathcal{Q}_L) \\
& + i\overline{q}_L\slashed{D}q_L + i\overline{b}_R\slashed{D}b_R + i\overline{t}_R\slashed{D}t_R \\
& - M_{10}\mathrm{Tr}(\overline{\mathcal{Q}}_R\mathcal{Q}_L) - yf\left(\Sigma^\dagger\overline{\mathcal{Q}}_R\mathcal{Q}_L\Sigma\right) + \mathrm{h.c.} \\
& - \lambda_t\overline{t}_R u_{1L} - \lambda_b\overline{b}_R d_{1L} - \lambda_q(\overline{T}_{4R}, \overline{d}_{4R})q_L + \mathrm{h.c.},
\end{aligned} \qquad (2.9)$$

with the covariant derivative

$$D_\mu\Sigma = \partial_\mu\Sigma - ig'B_\mu\Sigma(T_R^3 + X) - igW_\mu^a\Sigma T_L^a \qquad (2.10)$$

in terms of the SU(2)$_L$ and U(1)$_Y$ gauge fields W_μ^a and B_μ, respectively, with their corresponding couplings g and g'. The bilinear terms in the fermion fields lead to mass matrices for the $2/3$, $-1/3$ and $5/3$ charged fermions, when the Higgs field is shifted by its VEV $\langle H\rangle$, $H = \langle H\rangle + h$. The mass matrices can be diagonalized by means of a bi-unitary transformation. The 2-fermion couplings to one and two Higgs bosons are obtained by expanding the mass matrices in the interaction eigenstates up to first, respectively, second order in the Higgs field, and subsequent transformation into the mass eigenstate basis. The mass matrices and the coupling matrices of one Higgs boson to two bottom-like and top-like states can be found in ref. [119]. In the appendix A we give the coupling matrices for the 2-Higgs-2-fermion couplings and, for completeness, repeat the matrices given in ref. [119].

3   Next-to-leading order QCD corrections to Higgs pair production in composite Higgs models

The NLO QCD corrections to Higgs pair production in the SM have been computed in ref. [10] by applying the heavy top approximation, in which the heavy fermion loops are replaced by effective vertices of gluons to Higgs bosons. These can be obtained by means of the low-energy theorem (LET) [120–122]. The Higgs field is treated here as a
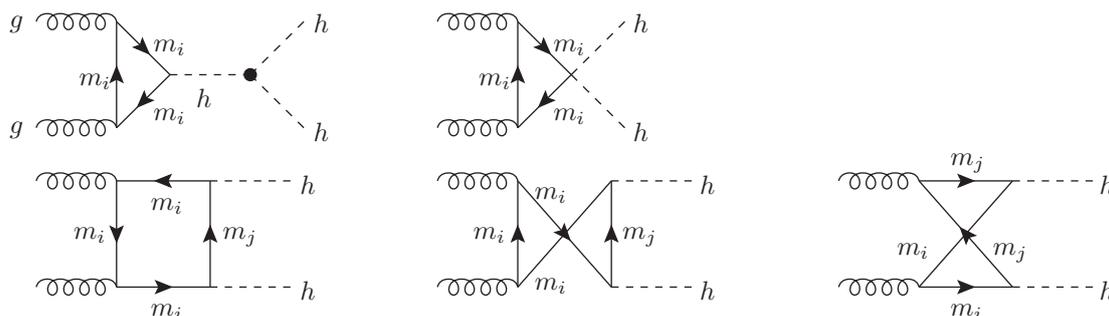
Figure 1. Generic Feynman diagrams contributing to $gg \to hh$ at LO, with n novel fermionic resonances, the top and the bottom quark with masses m_i $(i = 1, \ldots, n, t, b)$. The index j is introduced to indicate where different fermions can contribute in the loop.

background field, and the field-dependent mass of each heavy particle is taken into account in the gluon self-interactions at higher orders. The LET provides the zeroth order in an expansion in small external momenta. Since in Higgs pair production the requirements for such an expansion are not fulfilled sufficiently reliably, it fails to give accurate results for the cross section at LO [95]. In the context of composite Higgs models, the discrepancy between the LO cross section with full top quark mass dependence and the LO cross section in the LET approximation is even worse [88]. For relative higher order corrections the LET approximation should, however, become better, if the LO order cross section is taken into account with full mass dependence. This is because the dominant corrections given by the soft and collinear gluon corrections factorize from the LO cross section generating a part independent of the masses of the heavy loop particles relative to the LO cross section. This was confirmed in ref. [90] by including higher terms in the expansion of the cross section in small external momenta. Based on these findings, in this section we will give the NLO QCD corrections for Higgs pair production in composite Higgs models in the LET approach.

The expression of the LO gluon fusion into Higgs pairs in a composite Higgs model with heavy top partners has been given in [88].[7] It can be taken over here, by simply extending the sum to include also the bottom quark and its partners. We summarize here the most important features and refer to [88] for more details. The generic diagrams that contribute to the process at LO are depicted in figure 1. Besides the new 2-Higgs-2-fermion coupling $f\bar{f}hh$ the additional top and bottom partners in the loops have to be taken into account. These lead also to new box diagrams involving off-diagonal Yukawa couplings, with, respectively, the top and its heavy charge-2/3 partners or the bottom and its heavy partners of charge $-1/3$. The hadronic cross section is obtained by convolution with the parton distribution functions f_g of the gluon in the proton,

$$\sigma(pp \to hh + X) = \int_{\tau_0}^1 d\tau \int_\tau^1 \frac{dx}{x} f_g(x, \mu_F) f_g(\tau/x, \mu_F) \hat{\sigma}_{\text{LO}}(\tau s) , \qquad (3.1)$$

where s denotes the squared hadronic c.m. energy, μ_F the factorization scale and

$$\tau_0 = \frac{4m_h^2}{s} \qquad (3.2)$$

---

[7]For LO studies of Higgs pair production including contributions from vector-like quarks in Little(st) Higgs models, see e.g. refs. [123, 124].

in terms of the Higgs boson mass m_h. The partonic LO cross section can be cast into the form

$$\hat{\sigma}_{\rm LO}(gg \to hh) = \frac{\alpha_s^2(\mu_R)}{1024(2\pi)^3 \hat{s}^2} \int_{\hat{t}_-}^{\hat{t}_+} d\hat{t} \left[\Big| \sum_{q=t,b} \left(F_\triangle^{\rm LO} + F_\square^{\rm LO} \right) \Big|^2 + \Big| \sum_{q=t,b} G_\square^{\rm LO} \Big|^2 \right], \quad (3.3)$$

with the strong coupling constant α_s at the renormalization scale μ_R. We have introduced the Mandelstam variables

$$\hat{s} = \tau s = Q^2, \quad \hat{t} = m_h^2 - \frac{Q^2(1-\beta\cos\theta)}{2} \quad \text{and} \quad \hat{u} = m_h^2 - \frac{Q^2(1+\beta\cos\theta)}{2}, \quad (3.4)$$

in terms of the scattering angle θ in the partonic c.m. system with the invariant Higgs pair mass Q and the relative velocity

$$\beta = \sqrt{1 - \frac{4m_h^2}{Q^2}}. \quad (3.5)$$

The integration limits at $\cos\theta = \pm 1$ are given by

$$\hat{t}_\pm = m_h^2 - \frac{Q^2(1 \mp \beta)}{2}. \quad (3.6)$$

The form factors read

$$F_\triangle^{\rm LO} = \sum_{i=1}^{n_q} C_{i,\triangle} F_\triangle(m_i) \quad (3.7)$$

$$F_\square^{\rm LO} = \sum_{i=1}^{n_q} \sum_{j=1}^{n_q} \left(g_{h\bar{q}_i q_j}^2 F_\square(m_i, m_j) + g_{h\bar{q}_i q_j,5}^2 F_{\square,5}(m_i, m_j) \right) \quad (3.8)$$

$$G_\square^{\rm LO} = \sum_{i=1}^{n_q} \sum_{j=1}^{n_q} \left(g_{h\bar{q}_i q_j}^2 G_\square(m_i, m_j) + g_{h\bar{q}_i q_j,5}^2 G_{\square,5}(m_i, m_j) \right). \quad (3.9)$$

The triangle and box form factors $F_\triangle$, $F_\square$, $F_{\square,5}$, $G_\square$ and $G_{\square,5}$ can be found in the appendices of [88, 125].[8] The sum runs up to $n_t = 5$ for the top quark and its charge-2/3 partners and up to $n_b = 4$ in the bottom sector. The couplings are defined as

$$g_{h\bar{q}_i q_j} = \frac{1}{2}(G_{hqq,ij} + G_{hqq,ji}), \qquad g_{h\bar{q}_i q_j,5} = \frac{1}{2}(G_{hqq,ji} - G_{hqq,ij}) \quad (3.10)$$

and

$$g_{hh\bar{q}_i q_j} = (G_{hhqq,ij} + G_{hhqq,ji}), \quad (3.11)$$

where $G_{hqq,ij}$ and $G_{hhqq,ij}$ denote the (ith,jth) matrix elements of the coupling matrices in eq. (A.11) of the appendix. The triangle factor $C_{i,\triangle}$ reads in the MCHM10

$$C_{i,\triangle} = \frac{g_{hhh} g_{h\bar{q}_i q_i}}{Q^2 - m_h^2 + im_h\Gamma_h} + g_{hh\bar{q}_i q_i} \quad \text{with} \quad g_{hhh} = \frac{3m_h^2}{v} \frac{1-2\xi}{\sqrt{1-\xi}}, \quad (3.12)$$

---

[8]The form factors $F_\triangle, F_\square$ and $G_\square$ relate to those given in ref. [96] for the SM case as $F_\triangle(m) = \hat{s}/m \, F_\triangle^{\rm SM}(m)$, $F_\square = \hat{s}/m^2 F_\square^{\rm SM}(m)$ and $G_\square(m) = \hat{s}/m^2 G_\square^{\rm SM}(m)$.

as given in the MCHM5. In the SM and in the composite Higgs models MCHM4 and MCHM5 involving solely the Higgs non-linearities and no heavy fermionic resonances, no sum over heavy top and bottom partners contributes and only a sum over the top and bottom running in the loop has to be performed, i.e. $n_t = n_b = 1$, with $m_i = m_j = m_q$ and $q = t, b$, and hence also

$$g_{h\bar{q}_i q_j, 5} = 0 \qquad \text{for SM, MCHM4 and MCHM5.} \tag{3.13}$$

The Yukawa couplings read

$$g_{h\bar{q}q}^{\text{SM}} = \frac{m_q}{v}, \quad g_{h\bar{q}q}^{\text{MCHM4}} = g_{h\bar{q}q}^{\text{SM}} \sqrt{1 - \xi} \qquad \text{and} \qquad g_{h\bar{q}q}^{\text{MCHM5}} = g_{h\bar{q}q}^{\text{SM}} \frac{1 - 2\xi}{\sqrt{1 - \xi}}, \tag{3.14}$$

and for the 2-Higgs-2-fermion coupling we have

$$g_{hh\bar{q}q} = 0 \quad \text{in the SM and} \qquad g_{hh\bar{q}q}^{\text{MCHM4}} = -\xi \frac{m_q}{v^2} \quad \text{and} \quad g_{hh\bar{q}q}^{\text{MCHM5}} = -4\xi \frac{m_q}{v^2}, \tag{3.15}$$

while the Higgs self-coupling becomes

$$g_{hhh}^{\text{SM}} = \frac{3m_h^2}{v}, \quad g_{hhh}^{\text{MCHM4}} = g_{hhh}^{\text{SM}} \sqrt{1 - \xi} \quad \text{and} \quad g_{hhh}^{\text{MCHM5}} = g_{hhh}^{\text{SM}} \frac{1 - 2\xi}{\sqrt{1 - \xi}}. \tag{3.16}$$

The Feynman diagrams contributing to Higgs pair production at NLO QCD are shown in figure 2. The blob in the figure marks the effective vertices of gluons to Higgs boson(s). The first three Feynman diagrams show the virtual contributions. The remaining Feynman diagrams of figure 2 display the real corrections generically ordered by the initial states gg, gq and $q\bar{q}$. At NLO the cross section is then given by

$$\sigma_{\text{NLO}}(pp \to hh + X) = \sigma_{\text{LO}} + \Delta\sigma_{\text{virt}} + \Delta\sigma_{gg} + \Delta\sigma_{gq} + \Delta\sigma_{q\bar{q}}. \tag{3.17}$$

The individual contributions in eq. (3.17) read

$$\sigma_{\text{LO}} = \int_{\tau_0}^1 d\tau \frac{d\mathcal{L}^{gg}}{d\tau} \hat{\sigma}_{\text{LO}}(Q^2 = \tau s) \tag{3.18}$$

$$\Delta\sigma_{\text{virt}} = \frac{\alpha_s(\mu_R)}{\pi} \int_{\tau_0}^1 d\tau \frac{d\mathcal{L}^{gg}}{d\tau} \hat{\sigma}_{\text{LO}}(Q^2 = \tau s) \, C \tag{3.19}$$

$$\Delta\sigma_{gg} = \frac{\alpha_s(\mu_R)}{\pi} \int_{\tau_0}^1 d\tau \frac{d\mathcal{L}^{gg}}{d\tau} \int_{\tau_0/\tau}^1 \frac{dz}{z} \hat{\sigma}_{\text{LO}}(Q^2 = z\tau s) \left\{ -z P_{gg}(z) \log \frac{\mu_F^2}{\tau s} \right.$$
$$\left. -\frac{11}{2}(1 - z)^3 + 6[1 + z^4 + (1 - z)^4] \left(\frac{\log(1 - z)}{1 - z} \right)_+ \right\} \tag{3.20}$$

$$\Delta\sigma_{gq} = \frac{\alpha_s(\mu_R)}{\pi} \int_{\tau_0}^1 d\tau \sum_{q,\bar{q}} \frac{d\mathcal{L}^{gq}}{d\tau} \int_{\tau_0/\tau}^1 \frac{dz}{z} \hat{\sigma}_{\text{LO}}(Q^2 = z\tau s) \left\{ -\frac{z}{2} P_{gq}(z) \log \frac{\mu_F^2}{\tau s(1 - z)^2} \right.$$
$$\left. +\frac{2}{3}z^2 - (1 - z)^2 \right\} \tag{3.21}$$

$$\Delta\sigma_{q\bar{q}} = \frac{\alpha_s(\mu_R)}{\pi} \int_{\tau_0}^1 d\tau \sum_q \frac{d\mathcal{L}^{q\bar{q}}}{d\tau} \int_{\tau_0/\tau}^1 \frac{dz}{z} \hat{\sigma}_{\text{LO}}(Q^2 = z\tau s) \frac{32}{27}(1 - z)^3, \tag{3.22}$$

Virtual corrections:

gg induced real corrections:

gq induced real corrections:

$q\bar{q}$ induced real corrections:
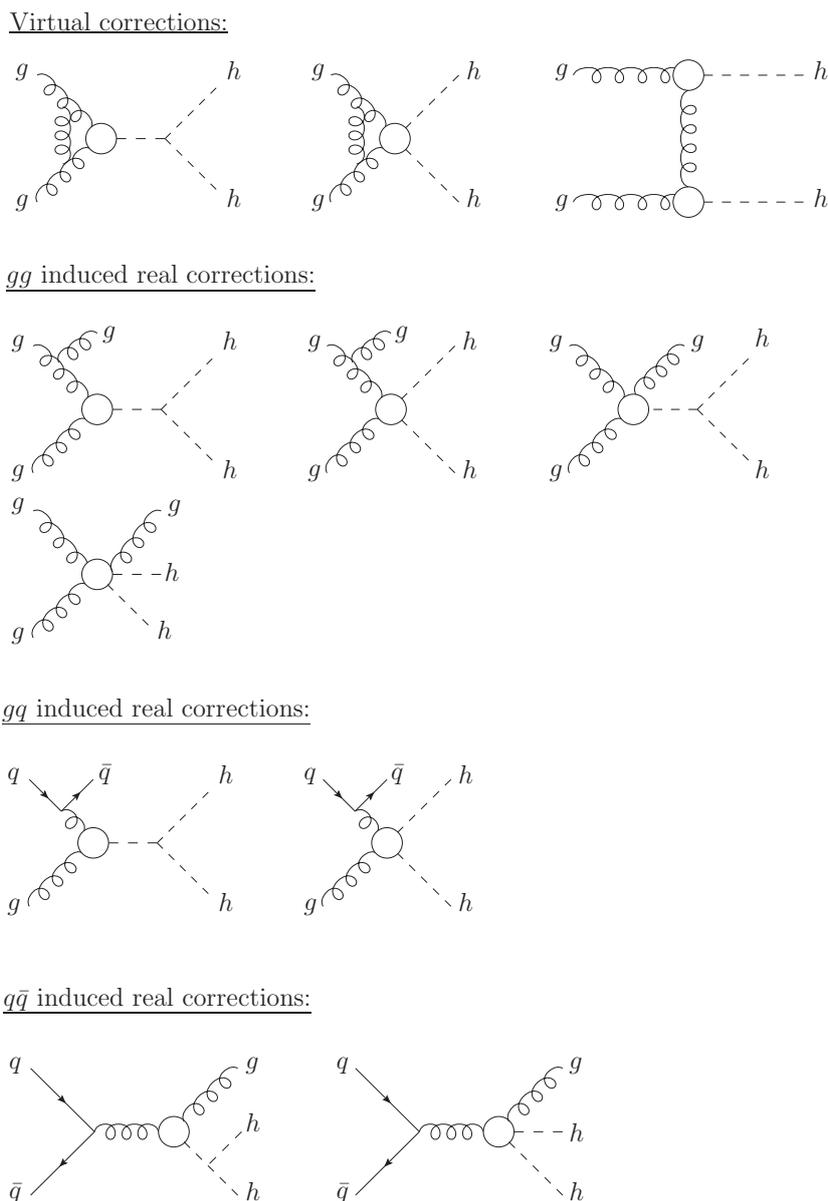
Figure 2. Generic Feynman diagrams contributing to the NLO QCD corrections to $gg \to hh$.

with the Altarelli-Parisi splitting functions given by [126]

$$P_{gg}(z) = 6 \left\{ \left(\frac{1}{1-z} \right)_+ + \frac{1}{z} - 2 + z(1-z) \right\} + \frac{33 - 2N_F}{6} \delta(1-z)$$

$$P_{gq}(z) = \frac{4}{3} \frac{1 + (1-z)^2}{z} \, , \tag{3.23}$$

and $N_F = 5$ in our case. The real corrections $\Delta\sigma_{gg}$, $\Delta\sigma_{gq}$ and $\Delta\sigma_{q\bar{q}}$ have straightforwardly been obtained from ref. [10] by replacing the LO cross section of the SM with the LO cross section for composite Higgs models. The calculation of $\Delta\sigma_{\text{virt}}$ is a bit more involved. While the first two diagrams factorize from the LO cross section and can hence directly be

taken over from the SM, the third diagram in figure 2 does not factorize and needs to be recalculated for the composite Higgs case. The virtual coefficient C is then found to be

$$
\begin{aligned}
C = \pi^2 + \frac{11}{2} + \frac{33 - 2N_F}{6} \log \frac{\mu_R^2}{Q^2} \\
+ \mathrm{Re} \frac{\int_{\hat{t}_-}^{\hat{t}_+} d\hat{t}\, \frac{4}{9}(g_{hgg}^{\mathrm{eff}})^2 \left\{ \left(F_\Delta^{\mathrm{LO}} + F_\square^{\mathrm{LO}} \right) - \frac{p_T^2}{2\hat{t}\hat{u}}(Q^2 - 2m_h^2)\, G_\square^{\mathrm{LO}} \right\}}{\int_{\hat{t}_-}^{\hat{t}_+} d\hat{t} \left[\left| \sum_{q=t,b} \left(F_\Delta^{\mathrm{LO}} + F_\square^{\mathrm{LO}} \right) \right|^2 + \left| \sum_{f=t,b} G_\square^{\mathrm{LO}} \right|^2 \right]}
\end{aligned}
\tag{3.24}
$$

with

$$
p_T^2 = \frac{(\hat{t} - m_h^2)(\hat{u} - m_h^2)}{Q^2} - m_h^2 \,.
\tag{3.25}
$$

The first line in eq. (3.24) corresponds to the NLO contribution from the first two diagrams in figure 2, while the second line corresponds to the NLO contribution from the third diagram of figure 2. The factor $(g_{hgg}^{\mathrm{eff}})^2$ stems from the two effective Higgs-gluon-gluon vertices in diagram 3 of figure 2. This vertex is obtained by integrating out all heavy loop particles in the loop-induced Higgs coupling to gluons defined in eq. (2.3) with $g_{hgg} \equiv g_{hgg}^{\mathrm{eff}}$ and

$$
g_{hgg}^{\mathrm{eff}} = \left(\sum_{i=1}^{n_t} \frac{g_{h\bar{q}_i q_i} v}{m_i} + \sum_{i=1}^{n_{\tilde{b}}} \frac{g_{h\bar{q}_i q_i} v}{m_i} \right) .
\tag{3.26}
$$

The first term is the sum over the normalized top quark and top partner couplings and the second term the sum over the normalized bottom partner couplings to the Higgs boson, excluding consistently the light bottom quark contribution from the loop. The composite Higgs cross sections for MCHM4, MCHM5 and for the composite Higgs model with heavy top and bottom partners, including the NLO corrections have been implemented in HPAIR.[9] In order to exemplify the impact of the NLO QCD corrections, we consider the simple case with the pure Higgs non-linearities only and the fermions transforming in the fundamental representation, i.e. the benchmark model MCHM5, see table 1. The coupling g_{hgg}^{eff} then reduces to $g_{hgg}^{\mathrm{MCHM5}} = (1 - 2\xi)/\sqrt{1 - \xi}$ and the remaining couplings are given in eqs. (3.13)–(3.16). We define the K-factors for the total cross section and the individual contributions as

$$
K = \frac{\sigma_{\mathrm{NLO}}}{\sigma_{\mathrm{LO}}} \qquad \text{and} \qquad K_i = \frac{\Delta\sigma_i}{\sigma_{\mathrm{LO}}} \,, \qquad i = \mathrm{virt}, gg, gq, q\bar{q} \,.
\tag{3.27}
$$

The cross section at LO is computed with the full quark mass dependences. As the NLO cross section in the LET approximation only includes top quark contributions,[10] at LO we consistently neglect also the bottom quark contributions, which in the SM amount to 1% for a 125 GeV Higgs boson. The c.m. energy $\sqrt{s} = 14\,\mathrm{TeV}$ and the top and bottom quark mass are set to $m_t = 173.2\,\mathrm{GeV}$ and $m_b = 4.75\,\mathrm{GeV}$, respectively. The cross sections are computed with the MSTW2008 PDF set [127]. The strong coupling constant is evaluated at the corresponding loop order with

$$
\alpha_s^{\mathrm{LO}}(M_Z) = 0.13939 \qquad \text{and} \qquad \alpha_s^{\mathrm{NLO}}(M_Z) = 0.12018 \,.
\tag{3.28}
$$

---

[9]See M. Spira's website, http://tiger.web.psi.ch/proglist.html.

[10]Note, that in MCHM5 we have no heavy top or bottom partners.
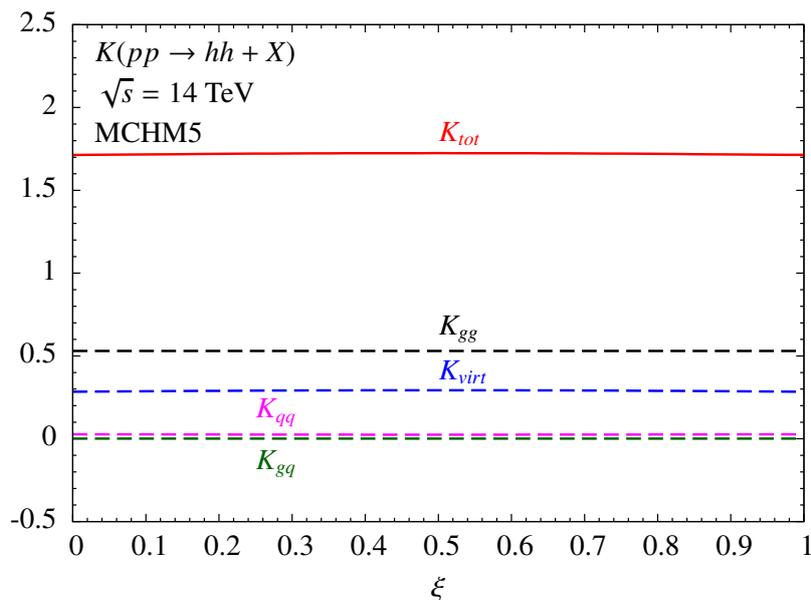
Figure 3. K-factors for the $pp \to hh + X$ cross section with $m_h = 125\,\text{GeV}$ in MCHM5 as a function of ξ for the scale choice $\mu_F = \mu_R = m_{hh}/2$ and the c.m. energy $\sqrt{s} = 14\,\text{TeV}$. The dashed lines show the individual contributions of the virtual contributions and the real corrections according to their initial states.

The renormalization and factorization scales are set to $\mu_R = \mu_F = m_{hh}/2$, where m_{hh} denotes the invariant Higgs pair mass. Figure 3 displays the results for the K-factors for the MCHM5 as a function of ξ. The solid line shows the total K-factor, the dashed lines are the individual contributions. As can be inferred from the plot, the real and virtual corrections of the gg initial state make up the bulk of the QCD corrections. The qg and the $q\bar{q}$ initiated real radiation diagrams only lead to a small correction. The K-factor is almost independent of ξ. In the real corrections, the Born cross section, which shows the only dependence on ξ, almost completely drops out numerically. For the virtual contributions some dependence on ξ may be expected. The virtual correction due to the constant term in C, i.e. the first line in eq. (3.24) does not develop any dependence on ξ, however, as it factorizes from the LO cross section. The dependence of ξ can only emerge from the second line in eq. (3.24), which, however, is numerically suppressed. This is already the case in the SM, where the corresponding term contributes less than 3% to $\Delta\sigma_{\text{virt}}$. This result also holds true for the case were the heavy quark partners are explicitly included. In composite Higgs models, the NLO QCD corrections to Higgs pair production can hence well be approximated by multiplying the full LO cross section of the composite Higgs model under consideration with the SM K-factor.

Figure 3 can also be obtained by using the results of ref. [103]. Note however, that the effects of heavy top and bottom partners in the effective field theory computation of ref. [103] have to be added to the top quark contribution, encoded into the Wilson coefficients in front of the operators $hG^{\mu\nu}G_{\mu\nu}$ and $hhG^{\mu\nu}G_{\mu\nu}$.

4 Numerical analysis of new physics effects in Higgs pair production via gluon fusion

Having derived the NLO QCD corrections, we can now turn to the analysis of NP effects in Higgs pair production. We assume that no NP is found before Higgs pair production becomes accessible. This means that we require deviations in the Higgs boson couplings with respect to the SM to be smaller than the projected sensitivities of the coupling measurements at an integrated luminosity of $300\,\mathrm{fb}^{-1}$ and $3000\,\mathrm{fb}^{-1}$, respectively. For the projected sensitivities we take the numbers reported in ref. [128]. Similar numbers can be found in refs. [129, 130]. In our analysis we focus on the most promising final states, given by $b\bar{b}\gamma\gamma$ and $b\bar{b}\tau^+\tau^-$ [14–17, 20].

We call Higgs pair production to be sensitive to NP if the difference between the number of signal events S in the considered NP model and the corresponding number S_{SM} in the SM exceeds a minimum of 3 statistical standard deviations, i.e.

$$S_{\mathrm{SM}} + \beta\sqrt{S_{\mathrm{SM}}} \leq S \qquad \text{or} \qquad S_{\mathrm{SM}} - \beta\sqrt{S_{\mathrm{SM}}} \geq S \qquad (4.1)$$

with $\beta = 3$ for a 3σ deviation. The signal events are obtained as

$$S = \sigma \cdot BR \cdot L \cdot A, \qquad (4.2)$$

where BR denotes the branching ratio into the respective final states, L the integrated luminosity and A the acceptance due to cuts applied on the cross section. The acceptances have been extracted from ref. [20] for the $b\bar{b}\gamma\gamma$ and $b\bar{b}\tau^+\tau^-$ final states. The acceptance for the BSM signal only changes slightly, as we explicitly checked.

In specific models, the correlations of the couplings will lead to stronger bounds on the parameters. In particular in the MCHM4 and MCHM5 as introduced in section 2, the only new parameter is ξ. The value of ξ can hence strongly be restricted by Higgs coupling measurements [131]. Based on the data for a c.m. energy of $\sqrt{s} = 7$ and $8\,\mathrm{TeV}$ at an integrated luminosity of 4.6-$4.8\,\mathrm{fb}^{-1}$ and $20.3\,\mathrm{fb}^{-1}$, respectively, ATLAS observes a 95% C.L. upper limit of $\xi < 0.12$ in the MCHM4 and of $\xi < 0.15$ in the MCHM5 [132]. This restricts the gluon fusion cross section for the MCHM4 to the range $40.06\,\mathrm{fb} \leq \sigma_{\mathrm{MCHM4}} \leq 44.55\,\mathrm{fb}$ and for the MCHM5 to $40.06\,\mathrm{fb} \leq \sigma_{\mathrm{MCHM5}} \leq 89.26\,\mathrm{fb}$. The value $\sigma = 40.06\,\mathrm{fb}$ corresponds to the SM cross section at NLO QCD for $m_t = 173.2\,\mathrm{GeV}$ and hence the MCHM4/MCHM5 value for $\xi = 0$. For the high luminosity options at the LHC we apply the projected estimates for the parameter ξ given in ref. [128],

$$\begin{aligned} \int \mathcal{L} = 300\,\mathrm{fb}^{-1} : \quad &\text{MCHM4: } 0.076 \\ &\text{MCHM5: } 0.068 \\ \int \mathcal{L} = 3000\,\mathrm{fb}^{-1} : \quad &\text{MCHM4: } 0.051 \\ &\text{MCHM5: } 0.015 \end{aligned} \qquad (4.3)$$

Based on these estimates, we give in table 2 the maximal values for the cross section times branching ratio. In the fourth and sixth columns we report whether the process within MCHM4, respectively, MCHM5 can be distinguished from the SM cross section by more than 3σ according to the criteria given in eq. (4.1) for $\beta = 3$. In the check of eq. (4.1) we took into account the slight change in the acceptance of the signal rate for the composite

		$\sigma_{b\bar{b}\gamma\gamma}$ [fb]	$\Delta_{3\sigma}$	$\sigma_{b\bar{b}\tau^{+}\tau^{-}}$ [fb]	$\Delta_{3\sigma}$
	$\xi = 0.12$ (LHC20.3)	0.119	no	3.26	no
MCHM4	$\xi = 0.076$ (LHC300)	0.114	no	3.13	no
	$\xi = 0.051$ (LHC3000)	0.112	no	3.07	no
	$\xi = 0.15$ (LHC20.3)	0.315	yes	5.35	yes
MCHM5	$\xi = 0.068$ (LHC300)	0.175	no	3.96	no
	$\xi = 0.015$ (LHC3000)	0.119	no	3.14	no

Table 2. Values of the cross section times branching ratio in the MCHM4 and MCHM5 for the maximal allowed values of ξ at 95% C.L. [132] and for the projected values at $\int \mathcal{L} = 300\,\text{fb}^{-1}$ and $\int \mathcal{L} = 3000\,\text{fb}^{-1}$ of ref. [128]. The fourth and sixth columns decide whether the Higgs production cross section will develop a deviation to the SM Higgs pair production cross section of more than 3σ according to the criteria of eq. (4.1).

Higgs models. Due to the coupling modifications and the new diagram from the 2-Higgs-2-fermion coupling the applied cuts in the analysis of ref. [20] affect the cross section in a slightly different way.

The table shows, that with the projected precision on ξ at high luminosities Higgs pair production in both MCHM4 and MCHM5 leads to cross sections too close to the SM value to be distinguishable from the SM case. Although with the present bounds on ξ Higgs pair production in MCHM5 differs by more than 3σ from the SM prediction, the corresponding cross section is too small to be measurable, so that first signs of NP through this process are precluded.

5   Numerical analysis for MCHM10

We consider the MCHM10 with one multiplet of fermionic resonances below the cut-off. In this model, with more than one parameter determining the Higgs coupling modifications, there is more freedom and a larger allowed parameter space (see ref. [119] for a thorough analysis). This implies, that the sensitivity on the Higgs couplings is less constrained. The numbers of the projected sensitivities are taken from table I in ref. [128]. Additionally, we need to take into account the bounds from the direct searches for new fermions. Currently, exotic new fermions with charge 5/3 are excluded up to masses of $m_\chi \leq 840\,\text{GeV}$ [133], bottom partners up to masses of $m_B \leq 900\,\text{GeV}$ [134] and top partners with masses of $m_T \leq 950\,\text{GeV}$ [135]. Note that the latter two limits on the masses depend on the branching ratios of the bottom and top partner, respectively. These limits are based on pair production of the new heavy fermions. First studies for single production of a new vector-like fermion were performed in refs. [136, 137] and can potentially be more important at large energies [138] but are more model-dependent. Due to this model dependence it is difficult to estimate the LHC reach on single production for our case. Hence we will only use the estimated reach on new vector-like fermions in pair production. In refs. [139–141] the potential reach of the LHC for charged-2/3 fermions, depending on their branching ratios is estimated. Following [141] we use the reach $m_T \lesssim 1.3$ TeV for $\int \mathcal{L} = 300\,\text{fb}^{-1}$

and $m_T \lesssim 1.5$ TeV for $\int \mathcal{L} = 3000\,\text{fb}^{-1}$. The potential reach for bottom partners is $m_B \lesssim 1$ TeV for $\int \mathcal{L} = 300\,\text{fb}^{-1}$ and $m_B \lesssim 1.5$ TeV for $\int \mathcal{L} = 3000\,\text{fb}^{-1}$ [142]. We estimate the additional sensitivity for the reach of exotic new fermions by multiplying the excluded cross section at $\sqrt{s} = 8$ TeV with [143]

$$ r = \sqrt{\frac{\sigma_{\text{BKG}}(14\text{ TeV})}{\sigma_{\text{BKG}}(8\text{ TeV})} \frac{L_{\text{LHC8}}}{L_{\text{LHC14}}}} \,, \tag{5.1} $$

where L_{LHC8} and L_{LHC14} denote the integrated luminosities of the LHC run at $\sqrt{s} = 8$ and 14 TeV, respectively. This implies a reach of $m_\chi \approx 1370$ GeV at $\int \mathcal{L} = 300\,\text{fb}^{-1}$ and $m_\chi \approx 1550$ GeV at $\int \mathcal{L} = 3000\,\text{fb}^{-1}$. For the background estimate we only considered the dominant background $t\bar{t}W^\pm$ [144]. The background cross section was computed with MadGraph5 [145, 146]. Although the assumption of stronger projections on the reach of new fermion masses of up to 2 TeV [147] will lead to a reduced number of points allowed by the constraints we are imposing, it will not change our final conclusion, as we checked explicitly. Note also that in composite Higgs models there is a connection between the Higgs boson mass and the fermionic resonances [148–153]. Reference [153] finds that the mass of the lightest top partner $m_{T_{\text{lightest}}}$ should be lighter than

$$ m_{T_{\text{lightest}}} \lesssim \frac{m_h \pi v}{m_t \sqrt{N_c} \sqrt{\xi}} \,, \tag{5.2} $$

with $N_c = 3$ denoting the number of colors. This bound, which is an estimate only on the upper mass value of the lightest top partner, will not further be taken into account.

For the analysis we performed a scan over the parameter space of the model by varying the parameters in the range[11]

$$ 0 \le \xi \le 1 \,, \quad 0 < \sin\phi_L \le 1 \,, \quad |y| < 4\pi \,, \quad 0 \le M_{10} \le 10\text{ TeV} \,. \tag{5.3} $$

We excluded points that do not fulfill $|V_{tb}| > 0.92$ [154] and the electroweak precision tests (EWPTs) at 99% C.L. using the results of ref. [119].

In figure 4 we show the NLO Higgs pair production cross section via gluon fusion as a function of ξ. The color code in the plots indicates whether the points are distinguishable from the SM according to the criteria given in eq. (4.1), with the blue points being distinguishable and the grey points not. The upper plots are for the $b\bar{b}\tau^+\tau^-$ final state, the lower plots for the $b\bar{b}\gamma\gamma$ final state, for $\int \mathcal{L} = 300\,\text{fb}^{-1}$ (left) and $\int \mathcal{L} = 3000\,\text{fb}^{-1}$ (right), respectively. The upper branch in the plots corresponds to the parameters $y < 0$ and $0 < R < 1$ with $R = (M_{10} + fy/2)/M_{10}$. This means that at LO of the mass matrix expansion in v/f, the lightest fermion partner originates from the SU(2) bi-doublet. The lower branch corresponds to the cases $y < 0$ and $R < 0$ as well as $y > 0$ implying $R > 1$.

The plots only show points for which we cannot see new physics anywhere else meaning we require that their deviations in the Higgs couplings that can be tested at the LHC are smaller than the expected sensitivities and that the masses of the new fermionic resonances

---

[11]Here ϕ_L is the rotation angle applied on the SU(2) bi-doublet for the diagonalization of the mass matrices at LO in v/f. It is related to the parameters of the model by $\tan\phi_L = \lambda_q/(M_{10} + fy/2)$.
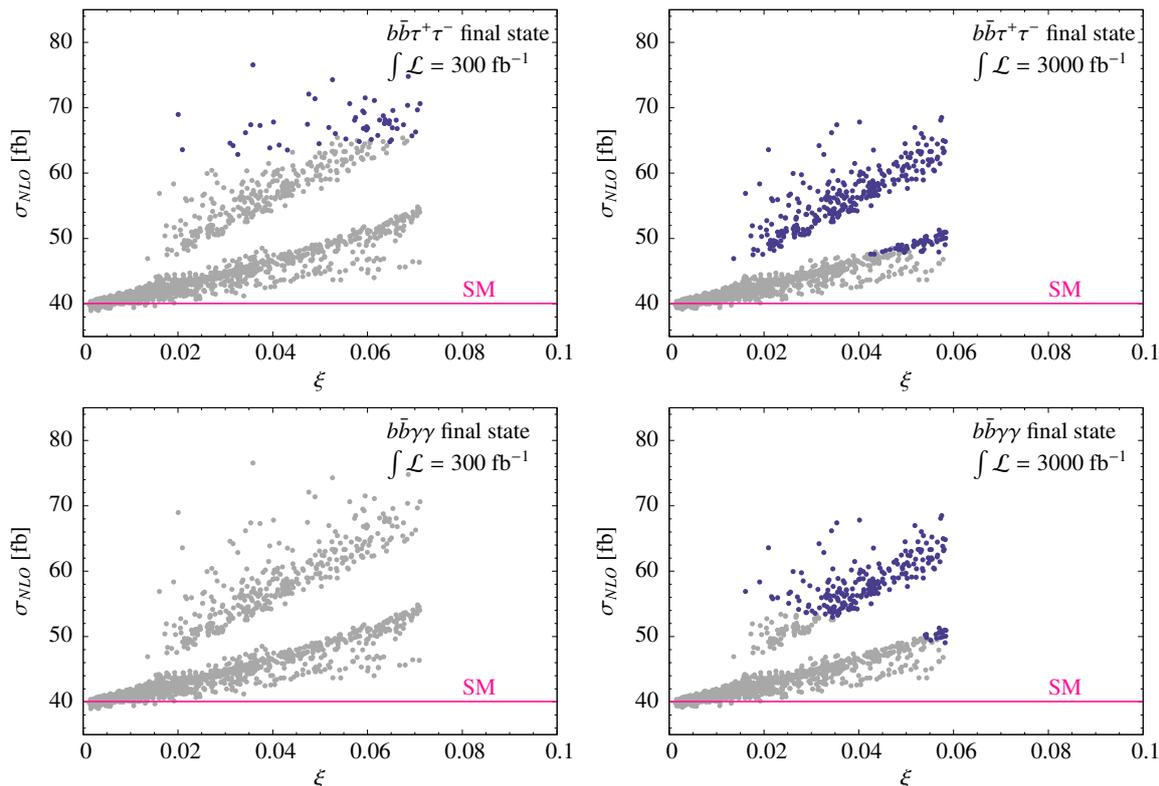
Figure 4. The NLO gluon fusion cross section into Higgs pairs in MCHM10 for a scan over ξ, y, $\sin\phi_L$ and M_{10}. All points pass the EWPTs and, for the respective luminosity, fulfill the projected direct search limits for new fermionic resonances at the LHC and allow only for deviations in the Higgs boson couplings that are smaller than the according expected sensitivity at the LHC. The blue points indicate that the composite Higgs pair production cross section can be distinguished from the SM one at 3σ in the $b\bar{b}\tau^+\tau^-$ final state (upper) and $b\bar{b}\gamma\gamma$ final state (lower) at an integrated luminosity $L = 300\,\text{fb}^{-1}$ (left) and $L = 3000$ fb^{-1} (right). The grey points cannot be distinguished from the SM at 3σ. The pink line is the SM prediction for the gluon fusion cross section at NLO.

are above the estimated reach of direct searches.[12] The requirement for only small deviations in the Higgs couplings directly restricts the possible values of ξ to be smaller than 0.071 and 0.059 for $\int\mathcal{L} = 300\,\text{fb}^{-1}$ and $\int\mathcal{L} = 3000\,\text{fb}^{-1}$, respectively. The value of ξ is restricted more strongly than in the MCHM4 due to the different coupling modifications, which, considering pure non-linearities, are for the Higgs-fermion couplings $(1-2\xi)/\sqrt{1-\xi}$ in MCHM10 and $\sqrt{1-\xi}$ in the MCHM4. Although the interplay of the various additional parameters in MCHM10 allows for some tuning in the Higgs-bottom (and also Higgs-top) coupling, this is not the case for the Higgs-tau coupling. Comparing the MCHM10 with the MCHM5, the Higgs-fermion couplings are modified in the same way, barring the effects from the additional fermions. The increased number of parameters due to the heavy fermions, however, allows for more freedom to accommodate the data, so that here the constraint is weaker in the MCHM10. The plots show that at $\int\mathcal{L} = 300$ fb^{-1} we cannot

---

[12]Note that we did not consider possible future results from flavour physics and/or the measurement of V_{tb} that could further restrict composite Higgs models.
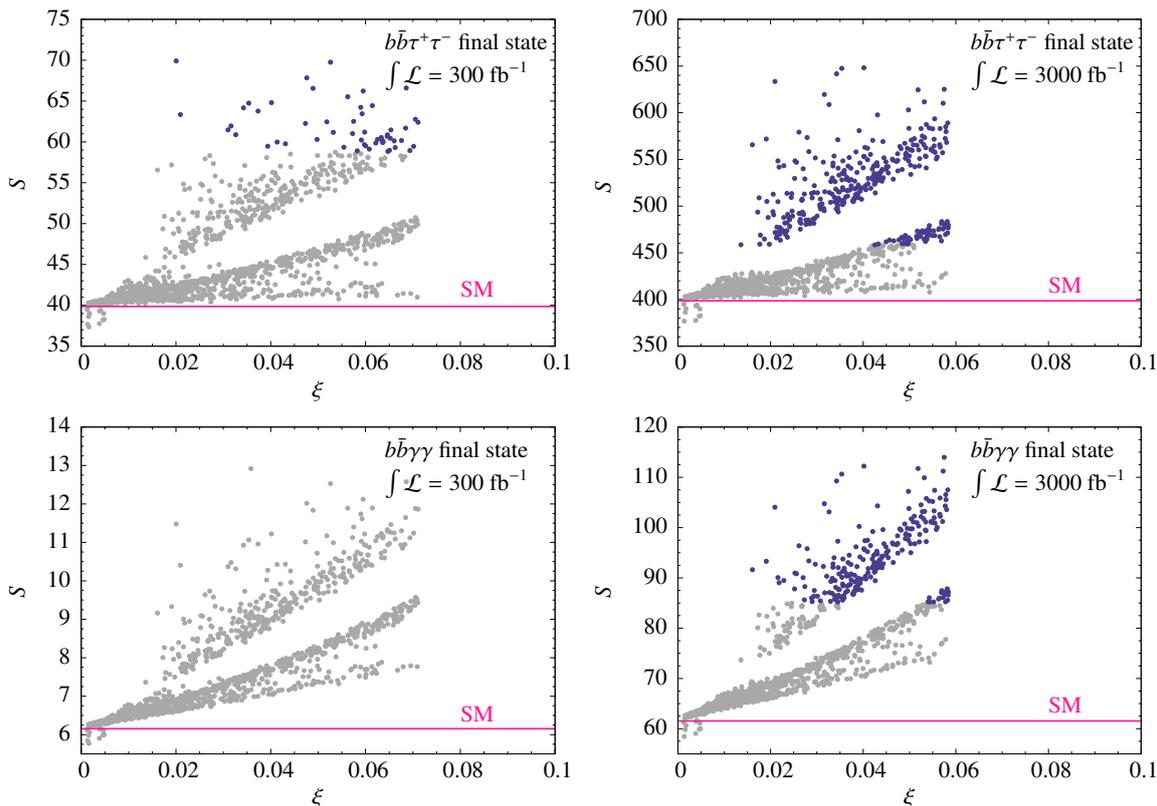
Figure 5. Number of signal events $S = \sigma_{\mathrm{NLO}} \cdot 2 \cdot \mathrm{BR}(h \to X) \cdot \mathrm{BR}(h \to Y) \cdot A \cdot L$ for NLO Higgs pair production in the final states $X = b\bar{b}$, $Y = \tau^+\tau^-$ (upper) and $X = b\bar{b}$, $Y = \gamma\gamma$ (lower) for an integrated luminosity of $L = 300\,\mathrm{fb}^{-1}$ (left) and $L = 3000\,\mathrm{fb}^{-1}$ (right), after multiplication with the individual acceptance A of the applied cuts, for the parameter points given in figure 4. The colour code is the same and the pink line refers to the NLO signal rate in the SM.

expect to discover NP for the first time in Higgs pair production in the $b\bar{b}\gamma\gamma$ final state, while in the $b\bar{b}\tau^+\tau^-$ final state NP could show up for the first time in Higgs pair production. For $\int \mathcal{L} = 3000\,\mathrm{fb}^{-1}$, we could find both in the $b\bar{b}\tau^+\tau^-$ and the $b\bar{b}\gamma\gamma$ final state points which lead to large enough deviations from the SM case to be sensitive to NP for the first time in Higgs pair production. These results can be explained with the increased signal rate in the cases that are sensitive, as can be inferred from figure 5. The plots show for the parameter points displayed in figure 4 the corresponding number of signal events for Higgs pair production in the $b\bar{b}\tau^+\tau^-$ and $b\bar{b}\gamma\gamma$ final states, respectively, after applying the acceptance of the cuts and multiplication with the two options of integrated luminosity. The blue points clearly deviate by more than 3σ from the SM curve.

6 Invariant mass distributions

Finally, in this section we discuss NP effects in invariant Higgs mass distributions. The measurement of distributions can give information on anomalous couplings [83] or the underlying ultraviolet source of NP [155]. Even though they are difficult to be measured

– 17 –
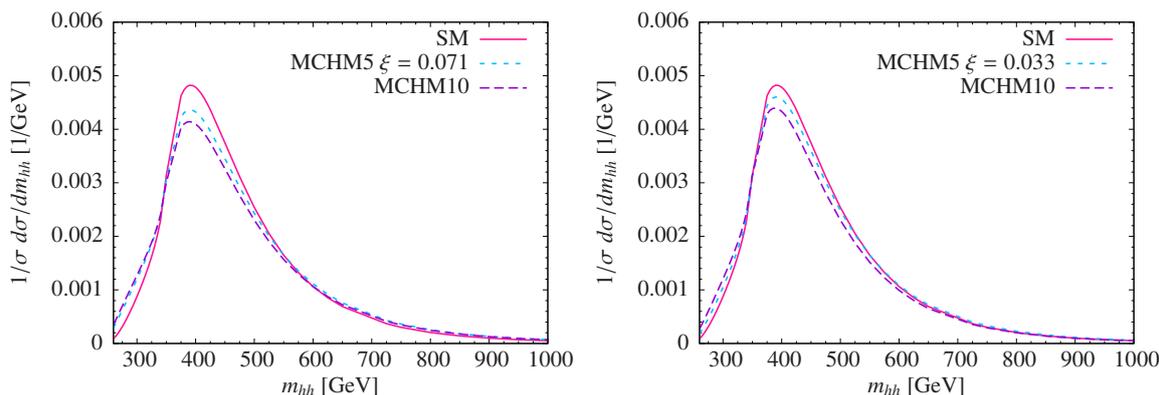
Figure 6. Normalized invariant mass distributions at NLO QCD for the SM (pink solid) and left: MCHM5 with $\xi = 0.071$ (blue dotted) and the MCHM10 with fermionic resonances for the parameter choice $\xi = 0.071$, $y = -7.292$, $\sin\phi_L = 0.551$ and $R = 0.615$ (violet dashed); right: MCHM5 with $\xi = 0.033$ (blued dotted) and the MCHM10 parameter choice $\xi = 0.033$, $y = -10.898$, $\sin\phi_L = 0.895$ and $R = 0.181$ (violet dashed).

due to the small numbers of signal events, they are important observables for the NP search. In the following we will show the impact of composite Higgs models on the distributions.

Figure 6 (left) shows the normalized invariant mass distributions for the MCHM5 with $\xi = 0.071$ (blue dotted) and the MCHM10 with one multiplet of fermionic resonances for the parameter choice $\xi = 0.071$, $y = -7.292$, $\sin\phi_L = 0.551$ and $R = 0.615$ (violet dashed) compared to the SM case (pink solid). In the right plot we show the same quantity, but for the MCHM5 with $\xi = 0.033$ (blue dotted) and the MCHM10 parameters $\xi = 0.033$, $y = -10.898$, $\sin\phi_L = 0.895$ and $R = 0.181$ (violet dashed) again compared to the SM (pink solid). The cross sections are computed at NLO. Note, however, that the shape of the invariant mass distributions hardly changes from LO to NLO, since in the LET approximation the LO cross section mainly factorizes from the NLO contributions, as discussed in section 3. The parameters have been chosen such that in the left plot we allow for a larger value of ξ, while the mass of the lightest top partner of $m_{T,\text{lightest}} = 5441$ GeV is much larger than compared to the case shown in the right plot with $m_{T,\text{lightest}} = 1636$ GeV. As can be inferred from these plots, the largest effect on the distributions originates from the pure non-linearities, i.e. the value of ξ, while the influence of the fermionic resonances on the shape of the invariant mass distributions is small. Note also that the main effect on the distributions emerges from the new $t\bar{t}hh$ coupling.

7 Conclusions

We presented the NLO QCD corrections to Higgs pair production via gluon fusion in the large quark mass approximation in composite Higgs models with and without new heavy fermionic resonances below the UV cut-off. We found that the K-factor of ~ 1.7 is basically independent of the value of ξ and of the details of the fermion spectrum, as the LO cross section dominantly factorizes. The K-factor can hence directly be taken over from the SM to a good approximation. The size of the absolute value of the cross section, however, sensitively depends on the Higgs non-linearities and on the fermion spectrum.

With the results of our NLO calculation, we furthermore addressed the question of whether NP could emerge for the first time in Higgs pair production, taking into account the constraints on the Higgs couplings to SM particles and from direct searches for new heavy fermions. We focused on composite Higgs models and found that in simple models where only the Higgs non-linearities are considered, we cannot expect to be sensitive to NP for the first time in Higgs pair production. In models with a multiplet of new fermions below the cut-off, it turned out that there are regions where NP could indeed be seen for the first time in Higgs pair production. The subsequent study of the NLO invariant mass distributions demonstrated, that while there is some sensitivity to the Higgs non-linearities mainly due to the new 2-Higgs-2-fermion coupling, the effect of the heavy fermions on the shape of the distributions is much weaker. By applying optimized cuts the sensitivity to new physics effects may possibly be increased in future.

Acknowledgments

A Masses and couplings

In the following we give the mass and coupling matrices for the composite Higgs model MCHM10 with heavy top and fermion partners, needed in the gluon fusion process into Higgs pairs. With the abbreviations

$$s_H \equiv \sin(H/f)\,, \qquad c_H \equiv \cos(H/f) \tag{A.1}$$

and

$$\tilde{m}_a \equiv \frac{1}{4} f y s_H^2 + M_{10}\,, \quad \tilde{m}_b \equiv \frac{1}{2} f y \left(1 - \frac{1}{2} s_H^2\right) + M_{10}\,, \quad \tilde{m}_c \equiv \frac{1}{2} f y c_H^2 + M_{10}\,, \tag{A.2}$$

the terms bilinear in the quark fields of eq. (2.9) read

$$-\mathcal{L}_{m_t} = \overline{\begin{pmatrix} t_L \\ u_L \\ u_{1L} \\ t_{4L} \\ T_{4L} \end{pmatrix}} \begin{pmatrix} 0 & 0 & 0 & 0 & \lambda_q \\ 0 & \tilde{m}_a & -\frac{1}{4} f y s_H^2 & -\frac{1}{4} f y c_H s_H & -\frac{1}{4} f y c_H s_H \\ \lambda_t & -\frac{1}{4} f y s_H^2 & \tilde{m}_a & \frac{1}{4} f y c_H s_H & \frac{1}{4} f y c_H s_H \\ 0 & -\frac{1}{4} f y c_H s_H & \frac{1}{4} f y c_H s_H & \tilde{m}_b & -\frac{1}{4} f y s_H^2 \\ 0 & -\frac{1}{4} f y c_H s_H & \frac{1}{4} f y c_H s_H & -\frac{1}{4} f y s_H^2 & \tilde{m}_b \end{pmatrix} \begin{pmatrix} t_R \\ u_R \\ u_{1R} \\ t_{4R} \\ T_{4R} \end{pmatrix} + \text{h.c.}\,, \tag{A.3}$$

$$-\mathcal{L}_{m_b} = \overline{\begin{pmatrix} b_L \\ d_L \\ d_{1L} \\ d_{4L} \end{pmatrix}} \begin{pmatrix} 0 & 0 & 0 & \lambda_q \\ 0 & \tilde{m}_a & -\frac{1}{4} f y s_H^2 & f y \frac{c_H s_H}{2\sqrt{2}} \\ \lambda_b & -\frac{1}{4} f y s_H^2 & \tilde{m}_a & -f y \frac{c_H s_H}{2\sqrt{2}} \\ 0 & f y \frac{c_H s_H}{2\sqrt{2}} & -f y \frac{c_H s_H}{2\sqrt{2}} & \tilde{m}_c \end{pmatrix} \begin{pmatrix} b_R \\ d_R \\ d_{1R} \\ d_{4R} \end{pmatrix} + \text{h.c.}\,, \tag{A.4}$$

and

$$-\mathcal{L}_{m_\chi} = \overline{\begin{pmatrix} \chi_L \\ \chi_{1L} \\ \chi_{4L} \end{pmatrix}} \begin{pmatrix} \tilde{m}_a & -\frac{1}{4} f y s_H^2 & f y \frac{c_H s_H}{2\sqrt{2}} \\ -\frac{1}{4} f y s_H^2 & \tilde{m}_a & -f y \frac{c_H s_H}{2\sqrt{2}} \\ f y \frac{c_H s_H}{2\sqrt{2}} & -f y \frac{c_H s_H}{2\sqrt{2}} & \tilde{m}_c \end{pmatrix} \begin{pmatrix} \chi_R \\ \chi_{1R} \\ \chi_{4R} \end{pmatrix} + \text{h.c.}\,. \tag{A.5}$$

Shifting the Higgs field in eqs. (A.3)–(A.5), encoded in s_H and c_H, respectively, by its VEV, i.e. $H = \langle H \rangle + h$, leads to the mass matrices M_t, M_b and M_χ. They can be diagonalized by a bi-unitary transformation

$$\left(U_L^{(t/b/\chi)} \right)^\dagger M_{(t/b/\chi)} U_R^{(t/b/\chi)} = M_{(t/b/\chi)}^{\mathrm{diag}}, \tag{A.6}$$

where $U_{L,R}^{(t/b/\chi)}$ denote the transformations that diagonalize the mass matrix in the top, bottom and charge-5/3 (χ) sector, respectively. Expansion of the mass matrices eqs. (A.3)–(A.5) in the interaction eigenstates up to first order in the Higgs field leads to the Higgs coupling matrices $\tilde{G}_{ht\bar{t}}$ to a pair of charge-2/3 quarks and $\tilde{G}_{hb\bar{b}}$ to a quark pair of charge $-1/3$, respectively, given by

$$-\mathcal{L}_{ht\bar{t}} = y\, h\, \overline{\begin{pmatrix} t_L \\ u_L \\ u_{1L} \\ t_{4L} \\ T_{4L} \end{pmatrix}} \underbrace{\begin{pmatrix} 0 & 0 & 0 & 0 & 0 \\ 0 & \frac{1}{2}s_H c_H & -\frac{1}{2}s_H c_H & \frac{1}{4}(2s_H^2-1) & \frac{1}{4}(2s_H^2-1) \\ 0 & -\frac{1}{2}s_H c_H & \frac{1}{2}s_H c_H & \frac{1}{4}(1-2s_H^2) & \frac{1}{4}(1-2s_H^2) \\ 0 & \frac{1}{4}(2s_H^2-1) & \frac{1}{4}(1-2s_H^2) & -\frac{1}{2}s_H c_H & -\frac{1}{2}s_H c_H \\ 0 & \frac{1}{4}(2s_H^2-1) & \frac{1}{4}(1-2s_H^2) & -\frac{1}{2}s_H c_H & -\frac{1}{2}s_H c_H \end{pmatrix}}_{\tilde{G}_{ht\bar{t}}/y} \begin{pmatrix} t_R \\ u_R \\ u_{1R} \\ t_{4R} \\ T_{4R} \end{pmatrix}_{H=\langle H \rangle} + \text{h.c.}, \tag{A.7}$$

$$-\mathcal{L}_{hb\bar{b}} = y\, h\, \overline{\begin{pmatrix} b_L \\ d_L \\ d_{1L} \\ d_{4L} \end{pmatrix}} \underbrace{\begin{pmatrix} 0 & 0 & 0 & 0 \\ 0 & \frac{1}{2}s_H c_H & -\frac{1}{2}s_H c_H & \frac{1}{2\sqrt{2}}(1-2s_H^2) \\ 0 & -\frac{1}{2}s_H c_H & \frac{1}{2}s_H c_H & \frac{1}{2\sqrt{2}}(2s_H^2-1) \\ 0 & \frac{1}{2\sqrt{2}}(1-2s_H^2) & \frac{1}{2\sqrt{2}}(2s_H^2-1) & -s_H c_H \end{pmatrix}}_{\tilde{G}_{hb\bar{b}}/y} \begin{pmatrix} b_R \\ d_R \\ d_{1R} \\ d_{4R} \end{pmatrix}_{H=\langle H \rangle} + \text{h.c.}. \tag{A.8}$$

Expansion up to second order in the Higgs field yields the 2-Higgs-2-fermion coupling matrices $\tilde{G}_{hht\bar{t}}$ and $\tilde{G}_{hhb\bar{b}}$, that can be cast into the form

$$-\mathcal{L}_{hht\bar{t}} = \frac{y}{2f}\, h\, \overline{\begin{pmatrix} t_L \\ u_L \\ u_{1L} \\ t_{4L} \\ T_{4L} \end{pmatrix}} \underbrace{\begin{pmatrix} 0 & 0 & 0 & 0 & 0 \\ 0 & (1-2s_H^2) & -(1-2s_H^2) & 2s_H c_H & 2s_H c_H \\ 0 & -(1-2s_H^2) & (1-2s_H^2) & -2s_H c_H & \frac{1}{4}(1-2s_H^2) \\ 0 & 2s_H c_H & -2s_H c_H & -(1-2s_H^2) & -(1-2s_H c_H) \\ 0 & 2s_H c_H & 2s_H c_H & -(1-2s_H^2) & -(1-2s_H^2) \end{pmatrix}}_{2f\,\tilde{G}_{hht\bar{t}}/y} \begin{pmatrix} t_R \\ u_R \\ u_{1R} \\ t_{4R} \\ T_{4R} \end{pmatrix}_{H=\langle H \rangle} + \text{h.c.}, \tag{A.9}$$

$$-\mathcal{L}_{hhb\bar{b}} = \frac{y}{2f}\, h\, \overline{\begin{pmatrix} b_L \\ d_L \\ d_{1L} \\ d_{4L} \end{pmatrix}} \underbrace{\begin{pmatrix} 0 & 0 & 0 & 0 \\ 0 & (1-2s_H^2) & -(1-2s_H^2) & -\sqrt{2}s_H c_H \\ 0 & -(1-2s_H^2) & (1-2s_H^2) & \sqrt{2}s_H c_H \\ 0 & -\sqrt{2}s_H c_H & \sqrt{2}s_H c_H & -2(1-2s_H^2) \end{pmatrix}}_{2f\,\tilde{G}_{hhb\bar{b}}/y} \begin{pmatrix} b_R \\ d_R \\ d_{1R} \\ d_{4R} \end{pmatrix}_{H=\langle H \rangle} + \text{h.c.}. \tag{A.10}$$

The coupling matrices in the mass eigenstate basis are obtained by rotation with the unitary matrices defined in eq. (A.6), i.e. ($q = t, b$)

$$(U_L^q)^\dagger \tilde{G}_{hq\bar{q}} U_R^q = G_{hq\bar{q}} \qquad \text{and} \qquad (U_L^q)^\dagger \tilde{G}_{hhq\bar{q}} U_R^q = G_{hhq\bar{q}}. \tag{A.11}$$

References

[1] ATLAS collaboration, *Observation of a new particle in the search for the Standard Model Higgs boson with the ATLAS detector at the LHC*, *Phys. Lett.* **B 716** (2012) 1 [`arXiv:1207.7214`] [INSPIRE].

[2] ATLAS collaboration, *Updated ATLAS results on the signal strength of the Higgs-like boson for decays into WW and heavy fermion final states*, ATLAS-CONF-2012-162 (2012).

[3] CMS collaboration, *Observation of a new boson at a mass of 125 GeV with the CMS experiment at the LHC*, *Phys. Lett.* **B 716** (2012) 30 [`arXiv:1207.7235`] [INSPIRE].

[4] CMS collaboration, *Combination of standard model Higgs boson searches and measurements of the properties of the new boson with a mass near 125 GeV*, CMS-PAS-HIG-12-045.

[5] P.W. Higgs, *Broken Symmetries and the Masses of Gauge Bosons*, *Phys. Rev. Lett.* **13** (1964) 508 [INSPIRE].

[6] P.W. Higgs, *Broken symmetries, massless particles and gauge fields*, *Phys. Lett.* **12** (1964) 132 [INSPIRE].

[7] F. Englert and R. Brout, *Broken Symmetry and the Mass of Gauge Vector Mesons*, *Phys. Rev. Lett.* **13** (1964) 321 [INSPIRE].

[8] G.S. Guralnik, C.R. Hagen and T.W.B. Kibble, *Global Conservation Laws and Massless Particles*, *Phys. Rev. Lett.* **13** (1964) 585 [INSPIRE].

[9] T.W.B. Kibble, *Symmetry breaking in nonAbelian gauge theories*, *Phys. Rev.* **155** (1967) 1554 [INSPIRE].

[10] S. Dawson, S. Dittmaier and M. Spira, *Neutral Higgs boson pair production at hadron colliders: QCD corrections*, *Phys. Rev.* **D 58** (1998) 115012 [`hep-ph/9805244`] [INSPIRE].

[11] A. Djouadi, W. Kilian, M. Mühlleitner and P.M. Zerwas, *Testing Higgs selfcouplings at e^+e^- linear colliders*, *Eur. Phys. J.* **C 10** (1999) 27 [`hep-ph/9903229`] [INSPIRE].

[12] A. Djouadi, W. Kilian, M. Mühlleitner and P.M. Zerwas, *Production of neutral Higgs boson pairs at LHC*, *Eur. Phys. J.* **C 10** (1999) 45 [`hep-ph/9904287`] [INSPIRE].

[13] M.M. Mühlleitner, *Higgs particles in the standard model and supersymmetric theories*, `hep-ph/0008127` [INSPIRE].

[14] U. Baur, T. Plehn and D.L. Rainwater, *Determining the Higgs boson selfcoupling at hadron colliders*, *Phys. Rev.* **D 67** (2003) 033003 [`hep-ph/0211224`] [INSPIRE].

[15] U. Baur, T. Plehn and D.L. Rainwater, *Examining the Higgs boson potential at lepton and hadron colliders: A comparative analysis*, *Phys. Rev.* **D 68** (2003) 033001 [`hep-ph/0304015`] [INSPIRE].

[16] U. Baur, T. Plehn and D.L. Rainwater, *Measuring the Higgs boson self coupling at the LHC and finite top mass matrix elements*, *Phys. Rev. Lett.* **89** (2002) 151801 [`hep-ph/0206024`] [INSPIRE].

[17] U. Baur, T. Plehn and D.L. Rainwater, *Probing the Higgs selfcoupling at hadron colliders using rare decays*, *Phys. Rev.* **D 69** (2004) 053004 [hep-ph/0310056] [INSPIRE].

[18] M.J. Dolan, C. Englert and M. Spannowsky, *Higgs self-coupling measurements at the LHC*, *JHEP* **10** (2012) 112 [arXiv:1206.5001] [INSPIRE].

[19] A. Papaefstathiou, L.L. Yang and J. Zurita, *Higgs boson pair production at the LHC in the* $b\bar{b}W^+W^-$ *channel*, *Phys. Rev.* **D 87** (2013) 011301 [arXiv:1209.1489] [INSPIRE].

[20] J. Baglio, A. Djouadi, R. Gröber, M.M. Mühlleitner, J. Quevillon and M. Spira, *The measurement of the Higgs self-coupling at the LHC: theoretical status*, *JHEP* **04** (2013) 151 [arXiv:1212.5581] [INSPIRE].

[21] F. Goertz, A. Papaefstathiou, L.L. Yang and J. Zurita, *Higgs Boson self-coupling measurements using ratios of cross sections*, *JHEP* **06** (2013) 016 [arXiv:1301.3492] [INSPIRE].

[22] W. Yao, *Studies of measuring Higgs self-coupling with* $HH \to b\bar{b}\gamma\gamma$ *at the future hadron colliders*, arXiv:1308.6302 [INSPIRE].

[23] A.J. Barr, M.J. Dolan, C. Englert and M. Spannowsky, *Di-Higgs final states augMT2ed — selecting hh events at the high luminosity LHC*, *Phys. Lett.* **B 728** (2014) 308 [arXiv:1309.6318] [INSPIRE].

[24] M.J. Dolan, C. Englert, N. Greiner and M. Spannowsky, *Further on up the road: hhjj production at the LHC*, *Phys. Rev. Lett.* **112** (2014) 101802 [arXiv:1310.1084] [INSPIRE].

[25] V. Barger, L.L. Everett, C.B. Jackson and G. Shaughnessy, *Higgs-Pair Production and Measurement of the Triscalar Coupling at LHC(8,14)*, *Phys. Lett.* **B 728** (2014) 433 [arXiv:1311.2931] [INSPIRE].

[26] D.E. Ferreira de Lima, A. Papaefstathiou and M. Spannowsky, *Standard model Higgs boson pair production in the* $(b\bar{b})(b\bar{b})$ *final state*, *JHEP* **08** (2014) 030 [arXiv:1404.7139] [INSPIRE].

[27] C. Englert, F. Krauss, M. Spannowsky and J. Thompson, *Di-Higgs phenomenology in* $t\bar{t}hh$: *The forgotten channel*, *Phys. Lett.* **B 743** (2015) 93 [arXiv:1409.8074] [INSPIRE].

[28] D. Wardrope, E. Jansen, N. Konstantinidis, B. Cooper, R. Falla and N. Norjoharuddeen, *Non-resonant Higgs-pair production in the* $b\bar{b}\ b\bar{b}$ *final state at the LHC*, *Eur. Phys. J.* **C 75** (2015) 219 [arXiv:1410.2794] [INSPIRE].

[29] Q. Li, Z. Li, Q.-S. Yan and X. Zhao, *Probe Higgs boson pair production via the* $3\ell 2j + \not{E}$ *mode*, *Phys. Rev.* **D 92** (2015) 014015 [arXiv:1503.07611] [INSPIRE].

[30] C.-T. Lu, J. Chang, K. Cheung and J.S. Lee, *An exploratory study of Higgs-boson pair production*, *JHEP* **08** (2015) 133 [arXiv:1505.00957] [INSPIRE].

[31] M.J. Dolan, C. Englert, N. Greiner, K. Nordstrom and M. Spannowsky, *hhjj production at the LHC*, *Eur. Phys. J.* **C 75** (2015) 387 [arXiv:1506.08008] [INSPIRE].

[32] Q.-H. Cao, Y. Liu and B. Yan, *Measuring Trilinear Higgs Coupling in WHH and ZHH Productions at the HL-LHC*, arXiv:1511.03311 [INSPIRE].

[33] J.K. Behr, D. Bortoletto, J.A. Frost, N.P. Hartland, C. Issever and J. Rojo, *Boosting Higgs pair production in the* $b\bar{b}b\bar{b}$ *final state with multivariate techniques*, arXiv:1512.08928 [INSPIRE].

[34] T. Plehn and M. Rauch, *The quartic Higgs coupling at hadron colliders*, *Phys. Rev.* **D 72** (2005) 053008 [`hep-ph/0507321`] [INSPIRE].

[35] G. Cynolter, E. Lendvai and G. Pocsik, *Resonance production of three neutral supersymmetric Higgs bosons at LHC*, *Acta Phys. Polon.* **B 31** (2000) 1749 [`hep-ph/0003008`] [INSPIRE].

[36] T. Binoth, S. Karg, N. Kauer and R. Ruckl, *Multi-Higgs boson production in the Standard Model and beyond*, *Phys. Rev.* **D 74** (2006) 113008 [`hep-ph/0608057`] [INSPIRE].

[37] CLIC PHYSICS WORKING GROUP collaboration, E. Accomando et al., *Physics at the CLIC multi-TeV linear collider*, `hep-ph/0412251` [INSPIRE].

[38] D. Chway, T.H. Jung, H.D. Kim and R. Dermisek, *Radiative Electroweak Symmetry Breaking Model Perturbative All the Way to the Planck Scale*, *Phys. Rev. Lett.* **113** (2014) 051801 [`arXiv:1308.0891`] [INSPIRE].

[39] C.J.C. Burges and H.J. Schnitzer, *Virtual Effects of Excited Quarks as Probes of a Possible New Hadronic Mass Scale*, *Nucl. Phys.* **B 228** (1983) 464 [INSPIRE].

[40] C.N. Leung, S.T. Love and S. Rao, *Low-Energy Manifestations of a New Interaction Scale: Operator Analysis*, *Z. Phys.* **C 31** (1986) 433 [INSPIRE].

[41] W. Buchmüller and D. Wyler, *Effective Lagrangian Analysis of New Interactions and Flavor Conservation*, *Nucl. Phys.* **B 268** (1986) 621 [INSPIRE].

[42] K. Hagiwara, S. Ishihara, R. Szalapski and D. Zeppenfeld, *Low-energy effects of new interactions in the electroweak boson sector*, *Phys. Rev.* **D 48** (1993) 2182 [INSPIRE].

[43] B. Grzadkowski, M. Iskrzynski, M. Misiak and J. Rosiek, *Dimension-Six Terms in the Standard Model Lagrangian*, *JHEP* **10** (2010) 085 [`arXiv:1008.4884`] [INSPIRE].

[44] J. Cao, D. Li, L. Shang, P. Wu and Y. Zhang, *Exploring the Higgs Sector of a Most Natural NMSSM and its Prediction on Higgs Pair Production at the LHC*, *JHEP* **12** (2014) 026 [`arXiv:1409.8431`] [INSPIRE].

[45] D. Buttazzo, F. Sala and A. Tesi, *Singlet-like Higgs bosons at present and future colliders*, *JHEP* **11** (2015) 158 [`arXiv:1505.05488`] [INSPIRE].

[46] P. Huang, A. Joglekar, B. Li and C.E.M. Wagner, *Probing the Electroweak Phase Transition at the LHC*, *Phys. Rev.* **D 93** (2016) 055049 [`arXiv:1512.00068`] [INSPIRE].

[47] R. Gröber and M. Mühlleitner, *Composite Higgs Boson Pair Production at the LHC*, *JHEP* **06** (2011) 020 [`arXiv:1012.1562`] [INSPIRE].

[48] S. Dawson, E. Furlan and I. Lewis, *Unravelling an extended quark sector through multiple Higgs production?*, *Phys. Rev.* **D 87** (2013) 014007 [`arXiv:1210.6663`] [INSPIRE].

[49] J. Cao, Z. Heng, L. Shang, P. Wan and J.M. Yang, *Pair Production of a 125 GeV Higgs Boson in MSSM and NMSSM at the LHC*, *JHEP* **04** (2013) 134 [`arXiv:1301.6437`] [INSPIRE].

[50] D.T. Nhung, M. Mühlleitner, J. Streicher and K. Walz, *Higher Order Corrections to the Trilinear Higgs Self-Couplings in the Real NMSSM*, *JHEP* **11** (2013) 181 [`arXiv:1306.3926`] [INSPIRE].

[51] U. Ellwanger, *Higgs pair production in the NMSSM at the LHC*, *JHEP* **08** (2013) 077 [`arXiv:1306.5541`] [INSPIRE].

[52] C. Han, X. Ji, L. Wu, P. Wu and J.M. Yang, *Higgs pair production with SUSY QCD correction: revisited under current experimental constraints*, *JHEP* **04** (2014) 003 [arXiv:1307.3790] [INSPIRE].

[53] M. Brucherseifer, R. Gavin and M. Spira, *Minimal supersymmetric Higgs boson self-couplings: Two-loop $O(\alpha_t\alpha_s)$ corrections*, *Phys. Rev.* **D 90** (2014) 117701 [arXiv:1309.3140] [INSPIRE].

[54] J.M. No and M. Ramsey-Musolf, *Probing the Higgs Portal at the LHC Through Resonant di-Higgs Production*, *Phys. Rev.* **D 89** (2014) 095031 [arXiv:1310.6035] [INSPIRE].

[55] A. Arhrib, P.M. Ferreira and R. Santos, *Are There Hidden Scalars in LHC Higgs Results?*, *JHEP* **03** (2014) 053 [arXiv:1311.1520] [INSPIRE].

[56] Z. Heng, L. Shang, Y. Zhang and J. Zhu, *Pair production of 125 GeV Higgs boson in the SM extension with color-octet scalars at the LHC*, *JHEP* **02** (2014) 083 [arXiv:1312.4260] [INSPIRE].

[57] E. Barradas-Guevara, O. Félix-Beltrán and E. Rodríguez-Jáuregui, *Trilinear self-couplings in an S_3 flavored Higgs model*, *Phys. Rev.* **D 90** (2014) 095001 [arXiv:1402.2244] [INSPIRE].

[58] A. Efrati and Y. Nir, *What if $\lambda_{hhh} \neq 3m_h^2/v$*, arXiv:1401.0935 [INSPIRE].

[59] J. Baglio, O. Eberhardt, U. Nierste and M. Wiebusch, *Benchmarks for Higgs Pair Production and Heavy Higgs boson Searches in the Two-Higgs-Doublet Model of Type II*, *Phys. Rev.* **D 90** (2014) 015008 [arXiv:1403.1264] [INSPIRE].

[60] B. Hespel, D. Lopez-Val and E. Vryonidou, *Higgs pair production via gluon fusion in the Two-Higgs-Doublet Model*, *JHEP* **09** (2014) 124 [arXiv:1407.0281] [INSPIRE].

[61] S.F. King, M. Mühlleitner, R. Nevzorov and K. Walz, *Discovery Prospects for NMSSM Higgs Bosons at the High-Energy Large Hadron Collider*, *Phys. Rev.* **D 90** (2014) 095014 [arXiv:1408.1120] [INSPIRE].

[62] V. Barger, L.L. Everett, C.B. Jackson, A.D. Peterson and G. Shaughnessy, *Measuring the two-Higgs doublet model scalar potential at LHC14*, *Phys. Rev.* **D 90** (2014) 095006 [arXiv:1408.2525] [INSPIRE].

[63] B. Yang, Z. Liu, N. Liu and J. Han, *Double Higgs production in the littlest Higgs Model with T-parity at high energy e^+e^- Colliders*, *Eur. Phys. J.* **C 74** (2014) 3203 [arXiv:1408.4295] [INSPIRE].

[64] L.-W. Chen, R.-Y. Zhang, W.-G. Ma, W.-H. Li, P.-F. Duan and L. Guo, *Probing the littlest Higgs model with T parity using di-Higgs events through Z_H-pair production at the LHC in NLO QCD*, *Phys. Rev.* **D 90** (2014) 054020 [arXiv:1409.1338] [INSPIRE].

[65] C.-Y. Chen, S. Dawson and I.M. Lewis, *Exploring resonant di-Higgs boson production in the Higgs singlet model*, *Phys. Rev.* **D 91** (2015) 035015 [arXiv:1410.5488] [INSPIRE].

[66] G.-L. Liu, X.-F. Guo, K. Wu, J. Jiang and P. Zhou, *Charged Higgs Pair Production at the LHC as a Probe of the Top-Seesaw Assisted Technicolor Models*, arXiv:1501.01714 [INSPIRE].

[67] V. Martín Lozano, J.M. Moreno and C.B. Park, *Resonant Higgs boson pair production in the $hh \to b\bar{b}\,WW \to b\bar{b}\ell^+\nu\ell^-\bar{\nu}$ decay channel*, *JHEP* **08** (2015) 004 [arXiv:1501.03799] [INSPIRE].

[68] S.I. Godunov, A.N. Rozanov, M.I. Vysotsky and E.V. Zhemchugov, *Extending the Higgs sector: an extra singlet*, *Eur. Phys. J.* **C 76** (2016) 1 [arXiv:1503.01618] [INSPIRE].

[69] L. Wu, J.M. Yang, C.-P. Yuan and M. Zhang, *Higgs self-coupling in the MSSM and NMSSM after the LHC Run 1*, *Phys. Lett.* **B 747** (2015) 378 [arXiv:1504.06932] [INSPIRE].

[70] M. Mühlleitner, D.T. Nhung and H. Ziesche, *The order $\mathcal{O}\left(\alpha_t\alpha_s\right)$ corrections to the trilinear Higgs self-couplings in the complex NMSSM*, *JHEP* **12** (2015) 034 [arXiv:1506.03321] [INSPIRE].

[71] S. Dawson and I.M. Lewis, *NLO corrections to double Higgs boson production in the Higgs singlet model*, *Phys. Rev.* **D 92** (2015) 094023 [arXiv:1508.05397] [INSPIRE].

[72] B. Batell, M. McCullough, D. Stolarski and C.B. Verhaaren, *Putting a Stop to di-Higgs Modifications*, *JHEP* **09** (2015) 216 [arXiv:1508.01208] [INSPIRE].

[73] Q.-H. Cao, B. Yan, D.-M. Zhang and H. Zhang, *Resolving the Degeneracy in Single Higgs Production with Higgs Pair Production*, *Phys. Lett.* **B 752** (2016) 285 [arXiv:1508.06512] [INSPIRE].

[74] I.F. Ginzburg, *Triple Higgs coupling in the most general 2HDM at SM-like scenario*, arXiv:1510.08270 [INSPIRE].

[75] W.-J. Zhang, W.-G. Ma, R.-Y. Zhang, X.-Z. Li, L. Guo and C. Chen, *Double Higgs boson production and decay in Randall-Sundrum model at hadron colliders*, *Phys. Rev.* **D 92** (2015) 116005 [arXiv:1512.01766] [INSPIRE].

[76] R. Costa, M. Mühlleitner, M.O.P. Sampaio and R. Santos, *Singlet Extensions of the Standard Model at LHC Run 2: Benchmarks and Comparison with the NMSSM*, arXiv:1512.05355 [INSPIRE].

[77] A. Agostini, G. Degrassi, R. Gröber and P. Slavich, *NLO-QCD corrections to Higgs pair production in the MSSM*, *JHEP* **04** (2016) 106 [arXiv:1601.03671] [INSPIRE].

[78] H. Zhou, Z. Heng and D. Li, *The properties of the Higgs bosons and Pair Production of the SM-like Higgs Boson in λ-SUSY at the LHC*, arXiv:1601.07288 [INSPIRE].

[79] V. Barger, T. Han, P. Langacker, B. McElrath and P. Zerwas, *Effects of genuine dimension-six Higgs operators*, *Phys. Rev.* **D 67** (2003) 115001 [hep-ph/0301097] [INSPIRE].

[80] R. Contino, M. Ghezzi, M. Moretti, G. Panico, F. Piccinini and A. Wulzer, *Anomalous Couplings in Double Higgs Production*, *JHEP* **08** (2012) 154 [arXiv:1205.5444] [INSPIRE].

[81] K. Nishiwaki, S. Niyogi and A. Shivaji, *ttH Anomalous Coupling in Double Higgs Production*, *JHEP* **04** (2014) 011 [arXiv:1309.6907] [INSPIRE].

[82] R. Contino, C. Grojean, D. Pappadopulo, R. Rattazzi and A. Thamm, *Strong Higgs Interactions at a Linear Collider*, *JHEP* **02** (2014) 006 [arXiv:1309.7038] [INSPIRE].

[83] C.-R. Chen and I. Low, *Double take on new physics in double Higgs boson production*, *Phys. Rev.* **D 90** (2014) 013018 [arXiv:1405.7040] [INSPIRE].

[84] F. Goertz, A. Papaefstathiou, L.L. Yang and J. Zurita, *Higgs boson pair production in the $D = 6$ extension of the SM*, *JHEP* **04** (2015) 167 [arXiv:1410.3471] [INSPIRE].

[85] A. Azatov, R. Contino, G. Panico and M. Son, *Effective field theory analysis of double Higgs boson production via gluon fusion*, *Phys. Rev.* **D 92** (2015) 035001 [arXiv:1502.00539] [INSPIRE].

[86] H.-J. He, J. Ren and W. Yao, *Probing new physics of cubic Higgs boson interaction via Higgs pair production at hadron colliders*, *Phys. Rev.* **D 93** (2016) 015003 [arXiv:1506.03302] [INSPIRE].

[87] L. Edelhäuser, A. Knochel and T. Steeger, *Applying EFT to Higgs Pair Production in Universal Extra Dimensions*, *JHEP* **11** (2015) 062 [arXiv:1503.05078] [INSPIRE].

[88] M. Gillioz, R. Gröber, C. Grojean, M. Mühlleitner and E. Salvioni, *Higgs Low-Energy Theorem (and its corrections) in Composite Models*, *JHEP* **10** (2012) 004 [arXiv:1206.7120] [INSPIRE].

[89] R.S. Gupta, H. Rzehak and J.D. Wells, *How well do we need to measure the Higgs boson mass and self-coupling?*, *Phys. Rev.* **D 88** (2013) 055024 [arXiv:1305.6397] [INSPIRE].

[90] J. Grigo, J. Hoff, K. Melnikov and M. Steinhauser, *On the Higgs boson pair production at the LHC*, *Nucl. Phys.* **B 875** (2013) 1 [arXiv:1305.7340] [INSPIRE].

[91] J. Grigo, J. Hoff, K. Melnikov and M. Steinhauser, *Higgs boson pair production at the LHC: top-quark mass effects at next-to-leading order*, PoS(RADCOR 2013)006 [arXiv:1311.7425] [INSPIRE].

[92] R. Frederix et al., *Higgs pair production at the LHC with NLO and parton-shower effects*, *Phys. Lett.* **B 732** (2014) 142 [arXiv:1401.7340] [INSPIRE].

[93] J. Grigo and J. Hoff, *Mass-corrections to double-Higgs production & TopoID*, PoS(LL2014)030 [arXiv:1407.1617] [INSPIRE].

[94] F. Maltoni, E. Vryonidou and M. Zaro, *Top-quark mass effects in double and triple Higgs production in gluon-gluon fusion at NLO*, *JHEP* **11** (2014) 079 [arXiv:1408.6542] [INSPIRE].

[95] E.W.N. Glover and J.J. van der Bij, *Higgs boson pair production via gluon fusion*, *Nucl. Phys.* **B 309** (1988) 282 [INSPIRE].

[96] T. Plehn, M. Spira and P.M. Zerwas, *Pair production of neutral Higgs particles in gluon-gluon collisions*, *Nucl. Phys.* **B 479** (1996) 46 [*Erratum ibid.* **B 531** (1998) 655] [hep-ph/9603205] [INSPIRE].

[97] D. de Florian and J. Mazzitelli, *Two-loop virtual corrections to Higgs pair production*, *Phys. Lett.* **B 724** (2013) 306 [arXiv:1305.5206] [INSPIRE].

[98] D. de Florian and J. Mazzitelli, *Higgs Boson Pair Production at Next-to-Next-to-Leading Order in QCD*, *Phys. Rev. Lett.* **111** (2013) 201801 [arXiv:1309.6594] [INSPIRE].

[99] J. Grigo, K. Melnikov and M. Steinhauser, *Virtual corrections to Higgs boson pair production in the large top quark mass limit*, *Nucl. Phys.* **B 888** (2014) 17 [arXiv:1408.2422] [INSPIRE].

[100] J. Grigo, J. Hoff and M. Steinhauser, *Higgs boson pair production: top quark mass effects at NLO and NNLO*, *Nucl. Phys.* **B 900** (2015) 412 [arXiv:1508.00909] [INSPIRE].

[101] D.Y. Shao, C.S. Li, H.T. Li and J. Wang, *Threshold resummation effects in Higgs boson pair production at the LHC*, *JHEP* **07** (2013) 169 [arXiv:1301.1245] [INSPIRE].

[102] D. de Florian and J. Mazzitelli, *Higgs pair production at next-to-next-to-leading logarithmic accuracy at the LHC*, *JHEP* **09** (2015) 053 [arXiv:1505.07122] [INSPIRE].

[103] R. Gröber, M. Mühlleitner, M. Spira and J. Streicher, *NLO QCD Corrections to Higgs Pair Production including Dimension-6 Operators*, *JHEP* **09** (2015) 092 [arXiv:1504.06577] [INSPIRE].

[104] H. Terazawa, K. Akama and Y. Chikashige, *Unified Model of the Nambu-Jona-Lasinio Type for All Elementary Particle Forces*, *Phys. Rev.* **D 15** (1977) 480 [INSPIRE].

[105] H. Terazawa, *Subquark Model of Leptons and Quarks*, *Phys. Rev.* **D 22** (1980) 184 [INSPIRE].

[106] D.B. Kaplan and H. Georgi, SU(2) × U(1) *Breaking by Vacuum Misalignment*, *Phys. Lett.* **B 136** (1984) 183 [INSPIRE].

[107] S. Dimopoulos and J. Preskill, *Massless Composites With Massive Constituents*, *Nucl. Phys.* **B 199** (1982) 206 [INSPIRE].

[108] T. Banks, *Constraints on* SU(2) × U(1) *breaking by vacuum misalignment*, *Nucl. Phys.* **B 243** (1984) 125 [INSPIRE].

[109] D.B. Kaplan, H. Georgi and S. Dimopoulos, *Composite Higgs Scalars*, *Phys. Lett.* **B 136** (1984) 187 [INSPIRE].

[110] H. Georgi, D.B. Kaplan and P. Galison, *Calculation of the Composite Higgs Mass*, *Phys. Lett.* **B 143** (1984) 152 [INSPIRE].

[111] H. Georgi and D.B. Kaplan, *Composite Higgs and Custodial* SU(2), *Phys. Lett.* **B 145** (1984) 216 [INSPIRE].

[112] M.J. Dugan, H. Georgi and D.B. Kaplan, *Anatomy of a Composite Higgs Model*, *Nucl. Phys.* **B 254** (1985) 299 [INSPIRE].

[113] G.F. Giudice, C. Grojean, A. Pomarol and R. Rattazzi, *The Strongly-Interacting Light Higgs*, *JHEP* **06** (2007) 045 [hep-ph/0703164] [INSPIRE].

[114] C. Degrande, J.M. Gerard, C. Grojean, F. Maltoni and G. Servant, *Probing Top-Higgs Non-Standard Interactions at the LHC*, *JHEP* **07** (2012) 036 [*Erratum ibid.* **03** (2013) 032] [arXiv:1205.1065] [INSPIRE].

[115] K. Agashe, R. Contino and A. Pomarol, *The minimal composite Higgs model*, *Nucl. Phys.* **B 719** (2005) 165 [hep-ph/0412089] [INSPIRE].

[116] R. Contino, L. Da Rold and A. Pomarol, *Light custodians in natural composite Higgs models*, *Phys. Rev.* **D 75** (2007) 055014 [hep-ph/0612048] [INSPIRE].

[117] D.B. Kaplan, *Flavor at SSC energies: A new mechanism for dynamically generated fermion masses*, *Nucl. Phys.* **B 365** (1991) 259 [INSPIRE].

[118] R. Contino, T. Kramer, M. Son and R. Sundrum, *Warped/composite phenomenology simplified*, *JHEP* **05** (2007) 074 [hep-ph/0612180] [INSPIRE].

[119] M. Gillioz, R. Gröber, A. Kapuvari and M. Mühlleitner, *Vector-like Bottom Quarks in Composite Higgs Models*, *JHEP* **03** (2014) 037 [arXiv:1311.4453] [INSPIRE].

[120] J.R. Ellis, M.K. Gaillard and D.V. Nanopoulos, *A Phenomenological Profile of the Higgs Boson*, *Nucl. Phys.* **B 106** (1976) 292 [INSPIRE].

[121] M.A. Shifman, A.I. Vainshtein, M.B. Voloshin and V.I. Zakharov, *Low-Energy Theorems for Higgs Boson Couplings to Photons*, *Sov. J. Nucl. Phys.* **30** (1979) 711 [INSPIRE].

[122] B.A. Kniehl and M. Spira, *Low-energy theorems in Higgs physics*, *Z. Phys.* **C 69** (1995) 77 [hep-ph/9505225] [INSPIRE].

[123] J.-J. Liu, W.-G. Ma, G. Li, R.-Y. Zhang and H.-S. Hou, *Higgs boson pair production in the little Higgs model at hadron collider*, *Phys. Rev.* **D 70** (2004) 015001 [hep-ph/0404171] [INSPIRE].

[124] L. Wang, W. Wang, J.M. Yang and H. Zhang, *Higgs-pair production in littlest Higgs model with T-parity*, *Phys. Rev.* **D 76** (2007) 017702 [arXiv:0705.3392] [INSPIRE].

[125] R. Gröber, *Aspects of Higgs Physics and New Physics at the LHC*, Ph.D. Thesis, Karlsruhe Institute of Technology (KIT), (2014).

[126] G. Altarelli and G. Parisi, *Asymptotic Freedom in Parton Language*, *Nucl. Phys.* **B 126** (1977) 298 [INSPIRE].

[127] A.D. Martin, W.J. Stirling, R.S. Thorne and G. Watt, *Parton distributions for the LHC*, *Eur. Phys. J.* **C 63** (2009) 189 [arXiv:0901.0002] [INSPIRE].

[128] C. Englert et al., *Precision Measurements of Higgs Couplings: Implications for New Physics Scales*, *J. Phys.* **G 41** (2014) 113001 [arXiv:1403.7191] [INSPIRE].

[129] M. Klute, R. Lafaye, T. Plehn, M. Rauch and D. Zerwas, *Measuring Higgs Couplings at a Linear Collider*, *Europhys. Lett.* **101** (2013) 51001 [arXiv:1301.1322] [INSPIRE].

[130] M.E. Peskin, *Estimation of LHC and ILC Capabilities for Precision Higgs Boson Coupling Measurements*, arXiv:1312.4974 [INSPIRE].

[131] S. Bock, R. Lafaye, T. Plehn, M. Rauch, D. Zerwas and P.M. Zerwas, *Measuring Hidden Higgs and Strongly-Interacting Higgs Scenarios*, *Phys. Lett.* **B 694** (2011) 44 [arXiv:1007.2645] [INSPIRE].

[132] ATLAS collaboration, *Constraints on New Phenomena via Higgs Coupling Measurements with the ATLAS Detector*, ATLAS-CONF-2014-010 (2014).

[133] ATLAS collaboration, *Search for vector-like B quarks in events with one isolated lepton, missing transverse momentum and jets at $\sqrt{s} = 8\,TeV$ with the ATLAS detector*, *Phys. Rev.* **D 91** (2015) 112011 [arXiv:1503.05425] [INSPIRE].

[134] CMS collaboration, *Search for pair-produced vector-like B quarks in proton-proton collisions at $\sqrt{s} = 8\,TeV$*, arXiv:1507.07129 [INSPIRE].

[135] ATLAS collaboration, *Search for production of vector-like quark pairs and of four top quarks in the lepton-plus-jets final state in pp collisions at $\sqrt{s} = 8\,TeV$ with the ATLAS detector*, *JHEP* **08** (2015) 105 [arXiv:1505.04306] [INSPIRE].

[136] ATLAS collaboration, *Search for pair and single production of new heavy quarks that decay to a Z boson and a third-generation quark in pp collisions at $\sqrt{s} = 8\,TeV$ with the ATLAS detector*, *JHEP* **11** (2014) 104 [arXiv:1409.5500] [INSPIRE].

[137] ATLAS collaboration, *Search for the production of single vector-like and excited quarks in the Wt final state in pp collisions at $\sqrt{s} = 8\,TeV$ with the ATLAS detector*, *JHEP* **02** (2016) 110 [arXiv:1510.02664] [INSPIRE].

[138] J.A. Aguilar-Saavedra, R. Benbrik, S. Heinemeyer and M. Pérez-Victoria, *Handbook of vectorlike quarks: Mixing and single production*, *Phys. Rev.* **D 88** (2013) 094010 [arXiv:1306.0572] [INSPIRE].

[139] S. Bhattacharya, J. George, U. Heintz, A. Kumar, M. Narain and J. Stupak, *Prospects for a Heavy Vector-Like Charge 2/3 Quark T search at the LHC with $\sqrt{s} = 14\,TeV$ and $33\,TeV$. "A Snowmass 2013 Whitepaper"*, arXiv:1309.0026 [INSPIRE].

[140] CMS collaboration, *Sensitivity study for ECFA: heavy vector-like charge 2/3 quarks*, CMS-PAS-FTR-13-026.

[141] CMS collaboration, *Projected Performance of an Upgraded CMS Detector at the LHC and HL-LHC: Contribution to the Snowmass Process*, arXiv:1307.7135 [INSPIRE].

[142] E.W. Varnes, *Vector-like B pair production at future pp colliders*, arXiv:1309.0788 [INSPIRE].

[143] A. Bharucha, S. Heinemeyer and F. von der Pahlen, *Direct Chargino-Neutralino Production at the LHC: Interpreting the Exclusion Limits in the Complex MSSM*, *Eur. Phys. J.* **C 73** (2013) 2629 [arXiv:1307.4237] [INSPIRE].

[144] CMS collaboration, *Search for T5/3 top partners in same-sign dilepton final state*, CMS-PAS-B2G-12-012.

[145] J. Alwall, M. Herquet, F. Maltoni, O. Mattelaer and T. Stelzer, *MadGraph 5: Going Beyond*, *JHEP* **06** (2011) 128 [arXiv:1106.0522] [INSPIRE].

[146] J. Alwall et al., *The automated computation of tree-level and next-to-leading order differential cross sections and their matching to parton shower simulations*, *JHEP* **07** (2014) 079 [arXiv:1405.0301] [INSPIRE].

[147] C. Delaunay, T. Flacke, J. Gonzalez-Fraile, S.J. Lee, G. Panico and G. Perez, *Light Non-degenerate Composite Partners at the LHC*, *JHEP* **02** (2014) 055 [arXiv:1311.2072] [INSPIRE].

[148] O. Matsedonskyi, G. Panico and A. Wulzer, *Light Top Partners for a Light Composite Higgs*, *JHEP* **01** (2013) 164 [arXiv:1204.6333] [INSPIRE].

[149] M. Redi and A. Tesi, *Implications of a Light Higgs in Composite Models*, *JHEP* **10** (2012) 166 [arXiv:1205.0232] [INSPIRE].

[150] D. Marzocca, M. Serone and J. Shu, *General Composite Higgs Models*, *JHEP* **08** (2012) 013 [arXiv:1205.0770] [INSPIRE].

[151] G. Panico, M. Redi, A. Tesi and A. Wulzer, *On the Tuning and the Mass of the Composite Higgs*, *JHEP* **03** (2013) 051 [arXiv:1210.7114] [INSPIRE].

[152] D. Pappadopulo, A. Thamm and R. Torre, *A minimally tuned composite Higgs model from an extra dimension*, *JHEP* **07** (2013) 058 [arXiv:1303.3062] [INSPIRE].

[153] A. Pomarol and F. Riva, *The Composite Higgs and Light Resonance Connection*, *JHEP* **08** (2012) 135 [arXiv:1205.6434] [INSPIRE].

[154] CMS collaboration, *Measurement of the single-top-quark t-channel cross section in pp collisions at $\sqrt{s} = 7$ TeV*, *JHEP* **12** (2012) 035 [arXiv:1209.4533] [INSPIRE].

[155] S. Dawson, A. Ismail and I. Low, *What's in the loop? The anatomy of double Higgs production*, *Phys. Rev.* **D 91** (2015) 115008 [arXiv:1504.05596] [INSPIRE].